

INTERIM REPORT

9-13-79

Accession No. 7909240682

Contract Program or Project Title:

Subject of this Document: "Effects of Non-Uniform Core Flow on Peak Cladding Temperature: MOXY/SCORE Sensitivity Calculations"

Type of Document: LOFT Technical Report

Author(s): S. C. Chang

Date of Document: August 1979

Responsible NRC Individual and NRC Office or Division: G. D. McPherson

This document was prepared primarily for preliminary or internal use. It has not received full review and approval. Since there may be substantive changes, this document should not be considered final.

H. P. Pearson
H. P. Pearson, Supervisor
for Information Processing
EG&G Idaho

Prepared for
U.S. Nuclear Regulatory Commission
Washington, D.C. 20555

NRC Fin #A6048
INTERIM REPORT

NRC Research and Technical
Assistance Report

997 355

LOFT TECHNICAL REPORT LTR 1111-61

AUGUST 15, 1979

USNRC P 394

EFFECTS OF NON-UNIFORM CORE FLOW
ON PEAK CLADDING TEMPERATURE: MOXY/SCORE
SENSITIVITY CALCULATIONS

S. C. Chang

NRC Research and Technical
Assistance Report



EG&G Idaho, Inc.



IDAHO NATIONAL ENGINEERING LABORATORY

DEPARTMENT OF ENERGY

IDAHO OPERATIONS OFFICE UNDER CONTRACT DE-AC07-76IDO1570

097 356

LOFT TECHNICAL REPORT
LOFT PROGRAM

FORM EG&G-229
(Rev. 12-78)

TITLE		REPORT NO.
Effects of Non-Uniform Core Flow on Peak Cladding Temperature: MOXY/SCORE Sensitivity Calculations		LTR 1111-61
AUTHOR	GWA NO.	
S. C. Chand	561353002	
PERFORMING ORGANIZATION	DATE	
Thermal Analysis	August 15, 1979	
LOFT APPROVAL		
<i>SW</i> <i>BLT</i>	<i>M. L. Russell</i>	

PP&TEB
Mgr

LEPD FD&AB Mgr PSB RSB P&CSB
Mgr Mgr Mgr Mgr

The MOXY/SCORE computer program is used to evaluate the potential effect on peak cladding temperature of selective cooling that may result from a nonuniform mass flux at the core boundaries during the blowdown phase of the LOFT L2-4 test.

The results of this study indicate that the effect of the flow nonuniformity at the core boundaries will be neutralized by a strong radial flow redistribution in the neighborhood of core boundaries. The implication is that the flow nonuniformity at the core boundaries has no significant effect on the thermal-hydraulic behavior and cladding temperature at the hot plane.

DISPOSITION OF RECOMMENDATIONS

No disposition required.

NRC Research and Technical
Assistance Report

997 357

INTERIM REPORT

Accession No. _____

Report No. LTR-1111-61

Contract Program or Project Title:

Subject of this Document: Effects of Non-Uniform Core Flow on Peak Cladding Temperature: MOXY/SCORE Sensitivity Calculations

Type of Document: LOFT Technical Report

Author(s): S. C. Chang

Date of Document: March 1979

Responsible NRC Individual and NRC Office or Division:

This document was prepared primarily for preliminary or internal use. It has not received full review and approval. Since there may be substantive changes, this document should not be considered final.

EG&G Idaho, Inc.
Idaho Falls, Idaho 83401

Prepared for the
U.S. Nuclear Regulatory Commission
and the U.S. Department of Energy
Idaho Operations Office
Under contract No. EY-76-C-07-1570
NRC FIN No.

INTERIM REPORT

997 353

ABSTRACT

The MOXY/SCORE computer program is used to evaluate the potential effect on peak cladding temperature of selective cooling that may result from a nonuniform mass flux at the core boundaries during the blowdown phase of the LOFT L2-4 test.

997 357

SUMMARY

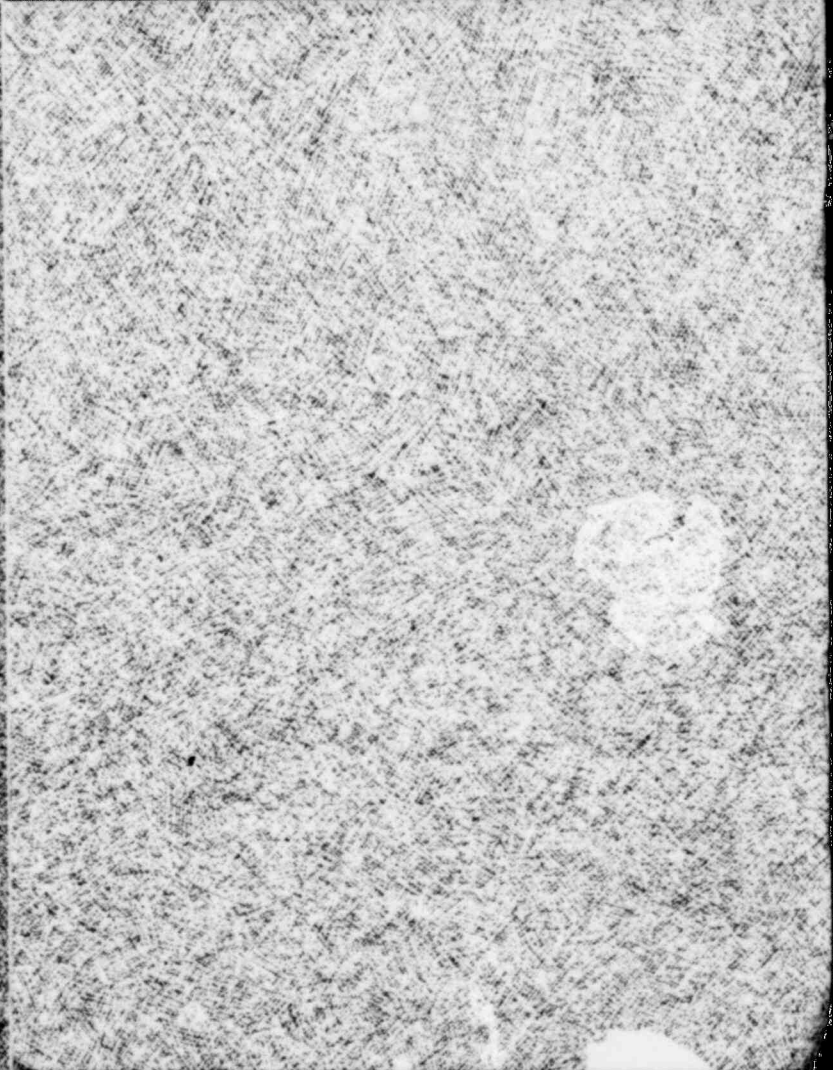
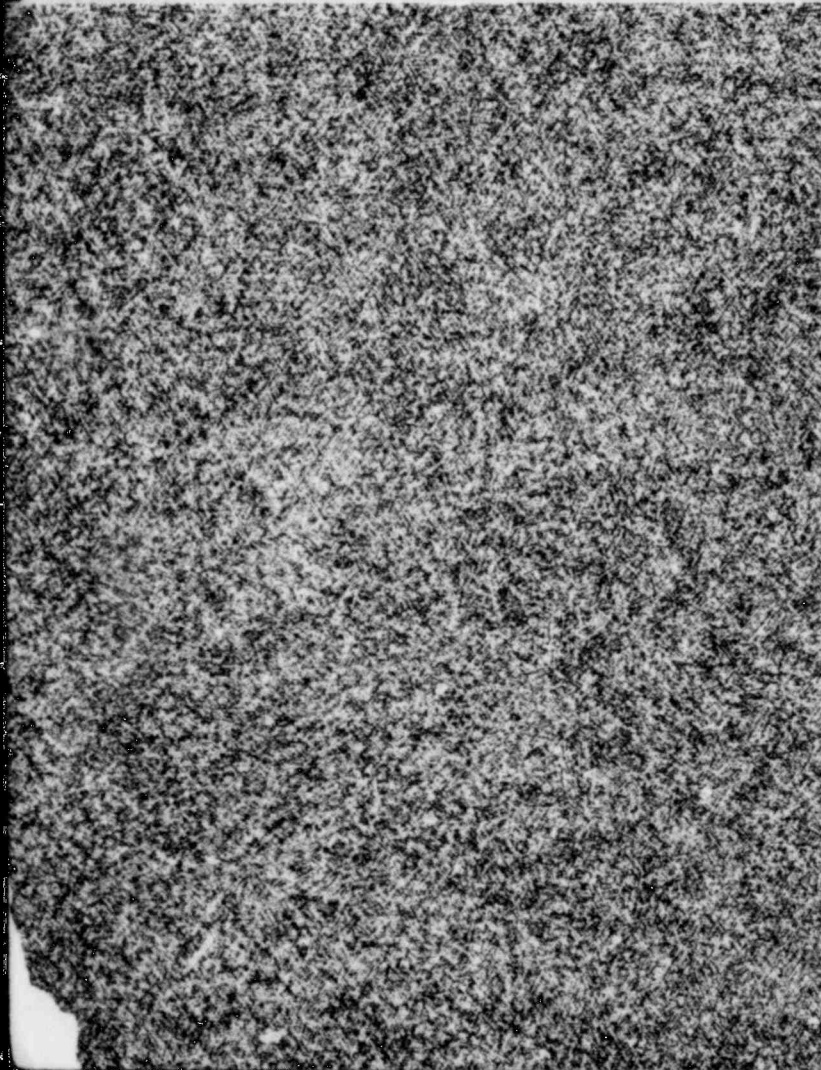
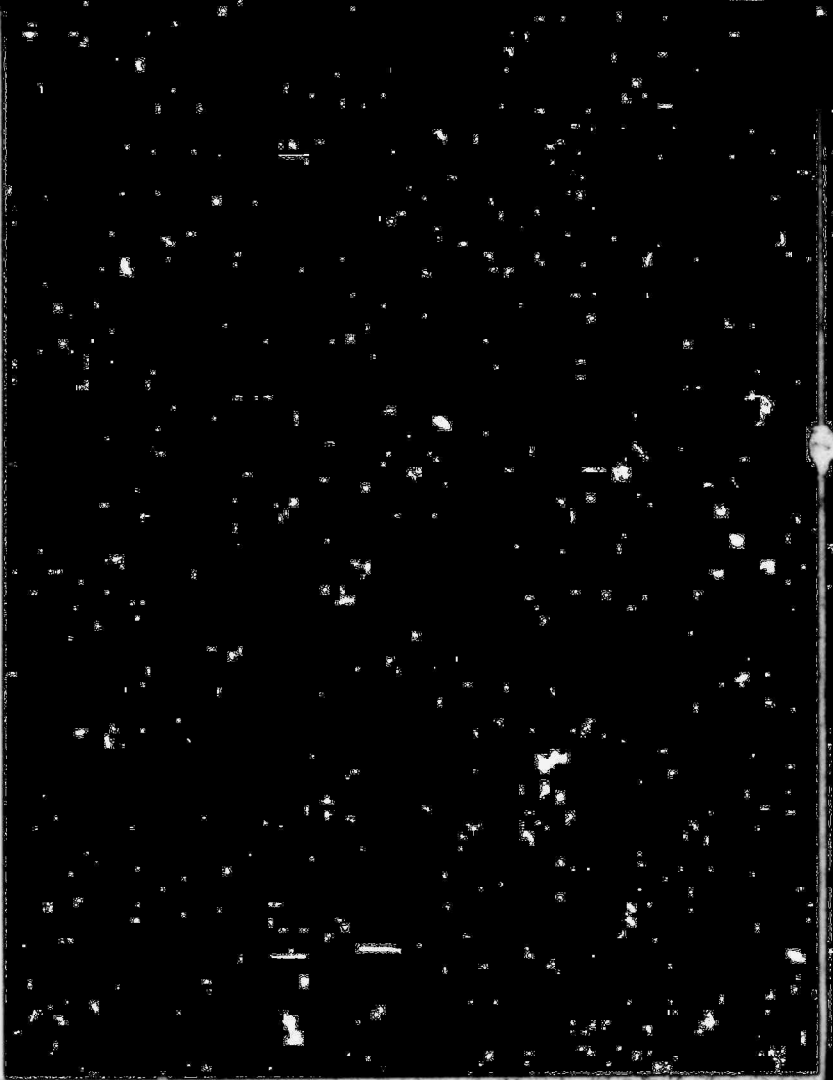
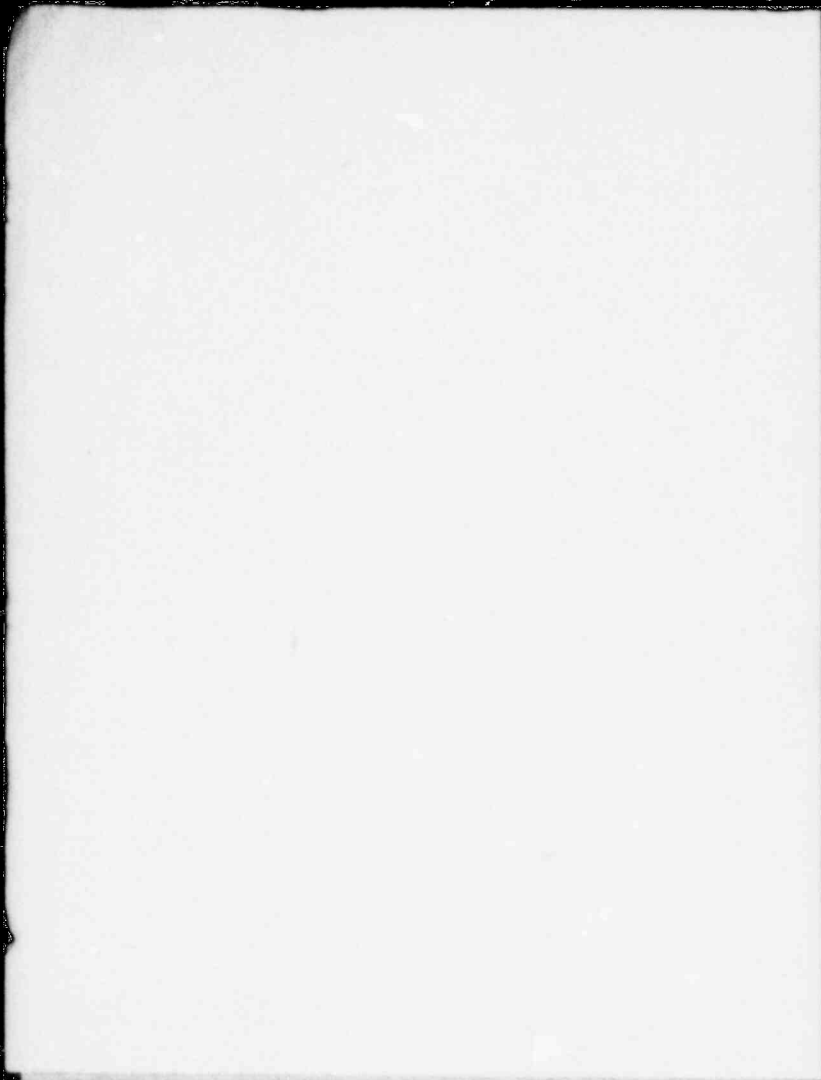
The purpose of this study is to evaluate the potential effects on peak cladding temperature that may result from a spatially nonuniform mass flux at the core boundaries during the blowdown phase of the LOFT L2-4 test.

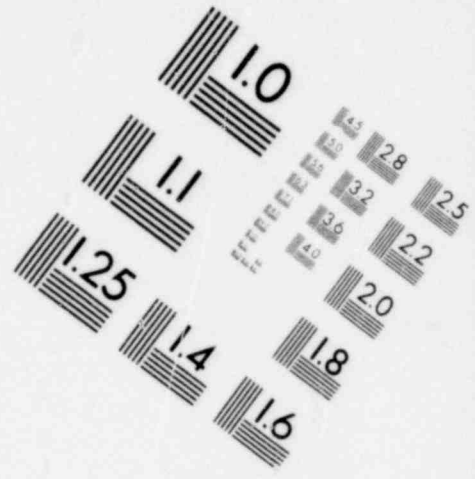
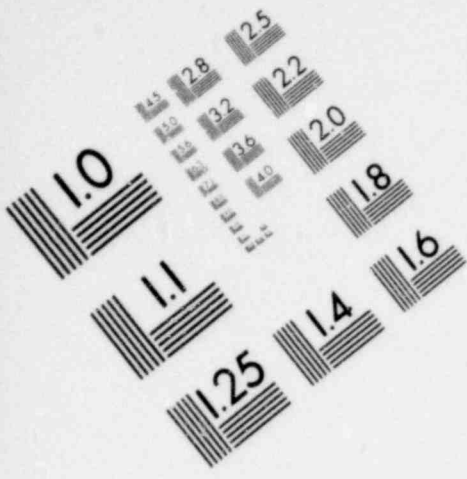
A direct approach to fulfill the goal of this study would involve the comparison and evaluation of the results of two computer calculations which simulate (1) a L2-4 test with uniform boundary mass flux distribution, and (2) a L2-4 test with actual boundary mass flux distribution, respectively. Unfortunately, this approach is not feasible because of the lack of test data that could provide actual flow distribution at the boundaries.

The alternate approach adopted in this study, is to carry out a sensitivity study of the L2-4 test peak cladding temperature as a function of the degree of flow nonuniformity at the core boundaries. The MOXY/SCORE computer program was used for this purpose.

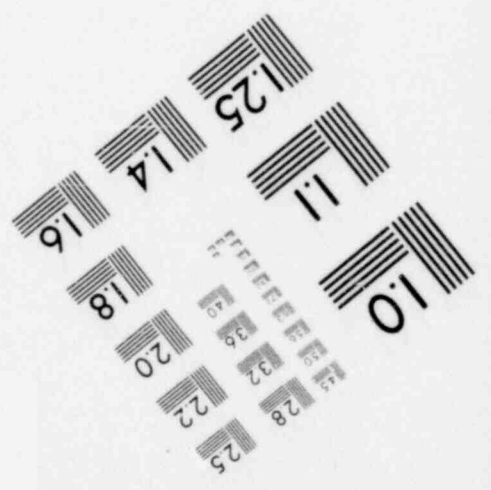
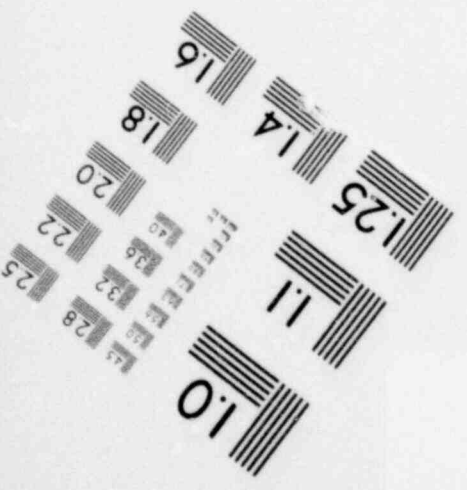
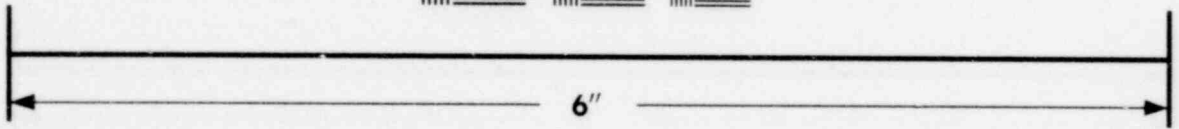
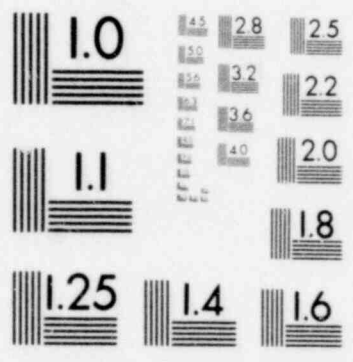
The results of this study indicate that the effect of the flow nonuniformity at the core boundaries will be neutralized by a strong radial flow redistribution in the neighborhood of core boundaries. The implication is that the flow nonuniformity at the core boundaries has no significant effect on the thermal-hydraulic behavior and cladding temperature at the hot plane.

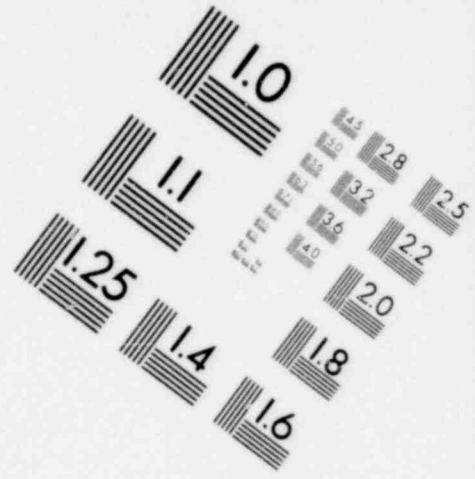
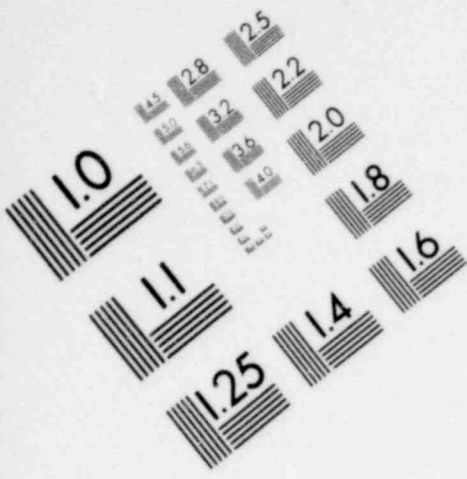
997 360



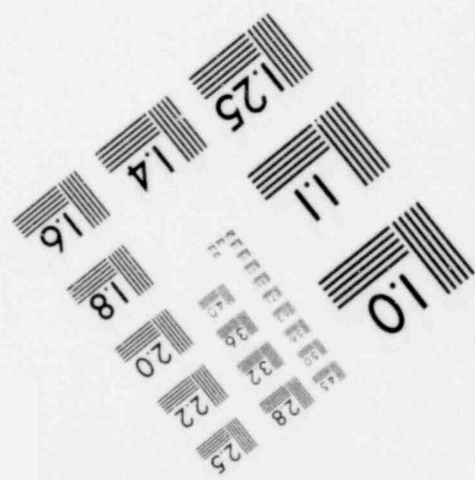
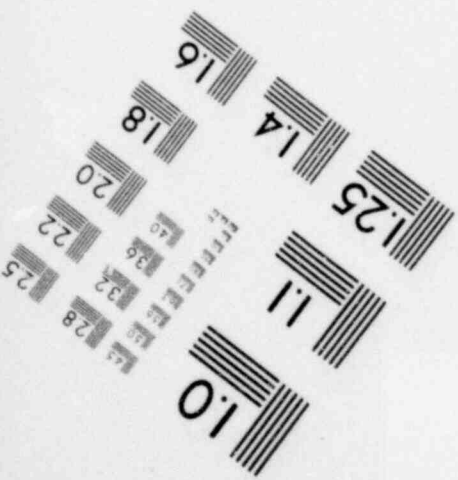
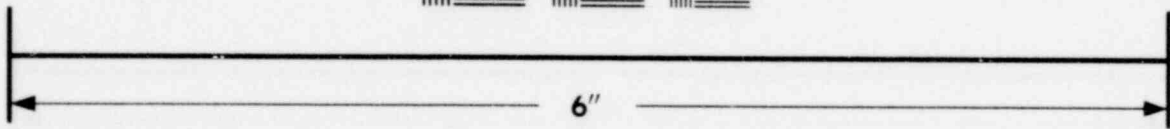
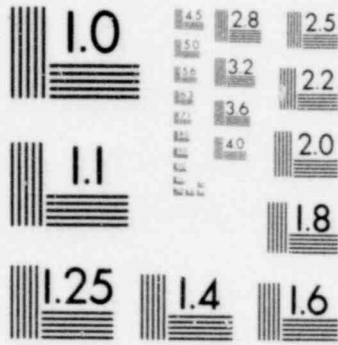


**IMAGE EVALUATION
TEST TARGET (MT-3)**





**IMAGE EVALUATION
TEST TARGET (MT-3)**



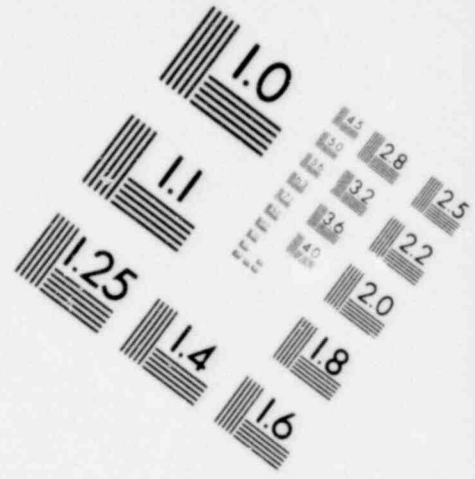
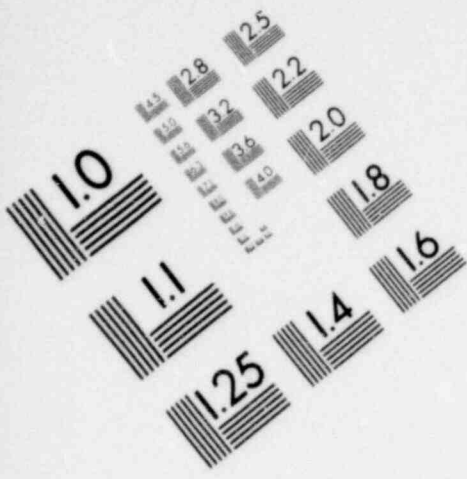
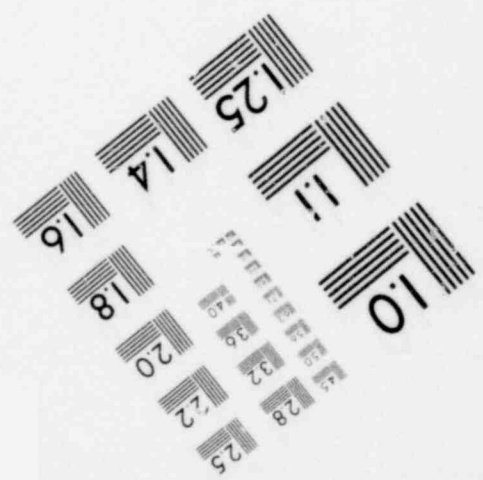
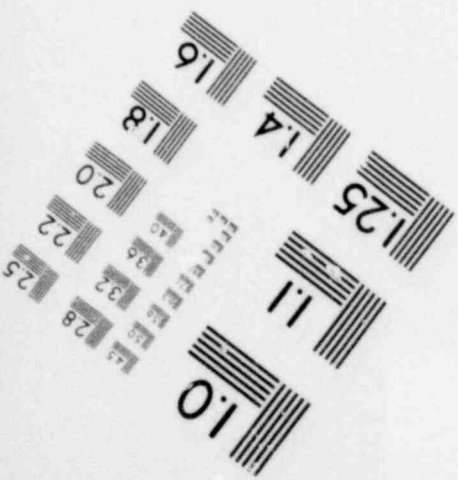
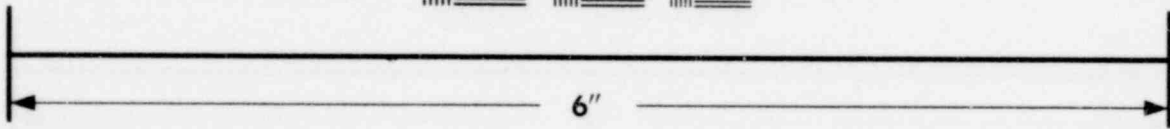
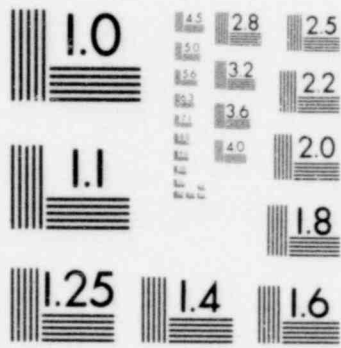


**IMAGE EVALUATION
TEST TARGET (MT-3)**



CONTENTS

SUMMARY. i⁺

I. INTRODUCTION. 1

II. BACKGROUND INFORMATION. 3

III. ANALYSIS APPROACH 7

IV. RESULTS AND ANALYSIS. 13

V. CONCLUSIONS AND RECOMMENDATIONS 30

APPENDIX A BOUNDARY CONDITION SPECIFICATIONS 32

APPENDIX B BOUNDARY AXIAL VELOCITY DISTRIBUTION. 34

REFERENCES 38

FIGURES

Fig. 1.	LOFT core cross-sectional view showing 16 flow channels for MOXY/SCORE model.	5
Fig. 2.	Fuel rod assembly axial cell arrangement for MOXY/SCORE model	6
Fig. 3.	Flow channel coordinates	10
Fig. 4.	Inlet boundary cell axial velocity (Run #1).	11
Fig. 5.	Comparison of x-velocities at the core inlet.	14
Fig. 6.	Comparison of x-velocities at first axial level	15
Fig. 7.	Comparison of x-velocities at second axial level.	16
Fig. 8.	Comparison of x-velocities at third axial level	17
Fig. 9.	Comparison of y-velocities at first axial level.	18
Fig. 10.	Comparison of x-velocities at ninth axial level	19
Fig. 11.	Comparison of fluid qualities at ninth axial level	20
Fig. 12.	Comparison of fluid densities at ninth axial level	21
Fig. 13.	Comparison of fluid temperatures at ninth axial level.	22
Fig. 14.	Comparison of fluid pressures at ninth axial level	23
Fig. 15.	Comparison of heat transfer modes at ninth axial level.	24
Fig. 16.	Comparison of convective heat fluxes at ninth axial level.	25
Fig. 17.	Comparison of radiation heat fluxes at ninth axial level.	26
Fig. 18.	Comparison of metal-water-reaction heat fluxes at ninth axial level.	27
Fig. 19.	Comparison of cladding temperatures at ninth axial level.	28
Fig. 20.	Values of $x_i(t)$ ($i = 1, 2, \dots, 16$) if $x_1(t) = 1.2$	35

998 002

- Fig. 21. Values of $x_i(t)$ ($i = 1, 2, \dots, 16$) if
 $x_1(t) = 1.6$ 36
- Fig. 22. Values of $x_i(t)$ ($i = 1, 2, \dots, 16$) if
 $x_1(t) = 2.0$ 37

998 003

I. INTRODUCTION

Computer program calculations provide a means to predict the fuel rod thermal response for the proposed loss-of-coolant experiments to be conducted as part of the first LOFT nuclear test series. These predictions serve as a basis for evaluating fuel reusability after each test and identifying conditions which may lead to potential cladding failure and release of radioactive materials.

An important part of these calculations, particularly for the more severe (high power) tests, is related to three-dimensional (3-D) coolant behavior in the core region and radiation heat transfer from the fuel rods. A previous study^[1] with the MOXY/SCORE computer program^[2] has shown that the crossflow in the core region does not influence peak cladding temperature by more than 25 K; however, radiation heat transfer effect is predicted to lower the peak cladding temperature by as much as 100 K. This study utilized coolant boundary conditions at the upper and lower core boundaries as calculated by RELAP4/MOD5 and further assumed the specified upper and lower core coolant conditions to be uniform.

It has been hypothesized that nonuniform coolant mass flux may exist at the core boundaries, particularly at the top of the core when reverse flow occurs. As a result, selective cooling may occur for the central module fuel rods.

To evaluate the potential selective cooling that may result from a nonuniform mass flux at the core boundaries, additional MOXY/SCORE calculations have been performed and the results are documented in this report. Section II discusses the boundary conditions which were chosen and utilized for the previous MOXY/SCORE calculations. It also provides other information which is common to both previous and current MOXY/SCORE calculations. Section III discusses how the boundary conditions were chosen to evaluate the effects of coolant

998 004

nonuniformity at the core boundaries. Section IV presents the results from calculations using nonuniform boundary conditions and compares them with those of the previous calculations. Section V summarizes conclusions and recommendations. Finally, Appendixes A & B are devoted to the discussion of the boundary conditions pertaining to current MOXY/SCORE calculations.

005

II. BACKGROUND INFORMATION

The current study is a complement to a previous study [1] dealing with the potential influence of crossflow and radiation heat transfer on LOFT LOCE behavior. Relevant information about the previous study is reviewed in this section, as follows:

- (a) As a prerequisite to any MOXY/SCORE calculations, one must specify, at the core boundaries, the temporal and spatial dependence of certain combinations of fluid axial velocity, fluid pressure, and fluid internal energy (see Table B-I of Reference 3.) An important restriction is that fluid axial velocity and pressure cannot be specified at the same boundary. As a result of these constraints and other considerations (explained in Appendix A), a particular set of boundary conditions was chosen for the previous MOXY/SCORE calculations. These boundary conditions are (1) fluid axial velocity and internal energy at the bottom of the core and (2) fluid pressure and internal energy at the top of the core. It was assumed that these boundary conditions are functions of time only and are spatially independent. These assumptions were made to simplify the original analysis and because of the lack of test data that could provide information regarding any potential spatial dependence of these boundary conditions.
- (b) Four MOXY/SCORE calculations were carried out in the previous study. They are:
 - (1) 3-D calculation with the radiation heat transfer mechanism turned on.

998 006
~~998 005~~

- (2) 3-D calculation with the radiation heat transfer mechanism turned off.
- (3) 1-D hot channel calculation.
- (4) 1-D peripheral channel calculation.

The results of these calculations were compared and used to evaluate the effects of crossflow and radiation heat transfer. Among these calculations, (1) provides the most realistic solution and will serve as the base case for the current calculations. This calculation, from now on, will be designated as Run #1.

- (c) The basic geometric model for Run #1 is identical to that for the current calculations. It can be described as follows:
 - (1) Figure 1 depicts the flow channels and Figure 2 shows the axial levels assumed to represent the LOFT reactor core.
 - (2) Referring to Figures 1 and 2, the fluid cell (FC) which is located at the n -th axial level in flow channel no. m will be designated as FC m - n . (FC m -0 and FC m -16 denote fluid cells at the lower and upper boundary axial levels, respectively.) Similarly, the corresponding fuel rod heat slab (FRHS) will be designated as FRHS m - n .

998 007

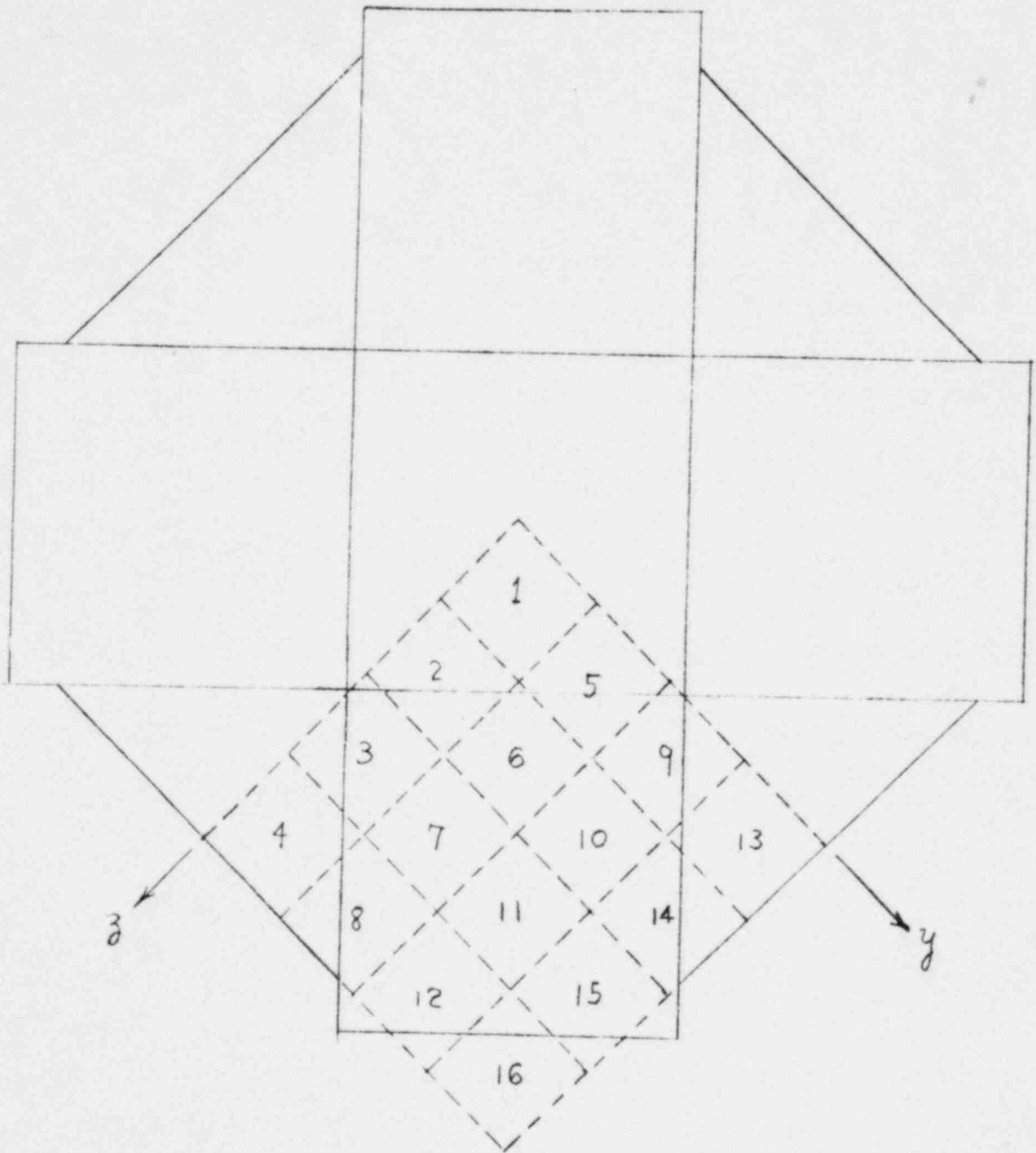


FIG. 1. LOFT CORE CROSS-SECTIONAL VIEW SHOWING
16 FLOW CHANNELS FOR MOXY/SCORE MODEL

998 003

$k = \text{FORM LOSS COEFFICIENT}^{[4]}$

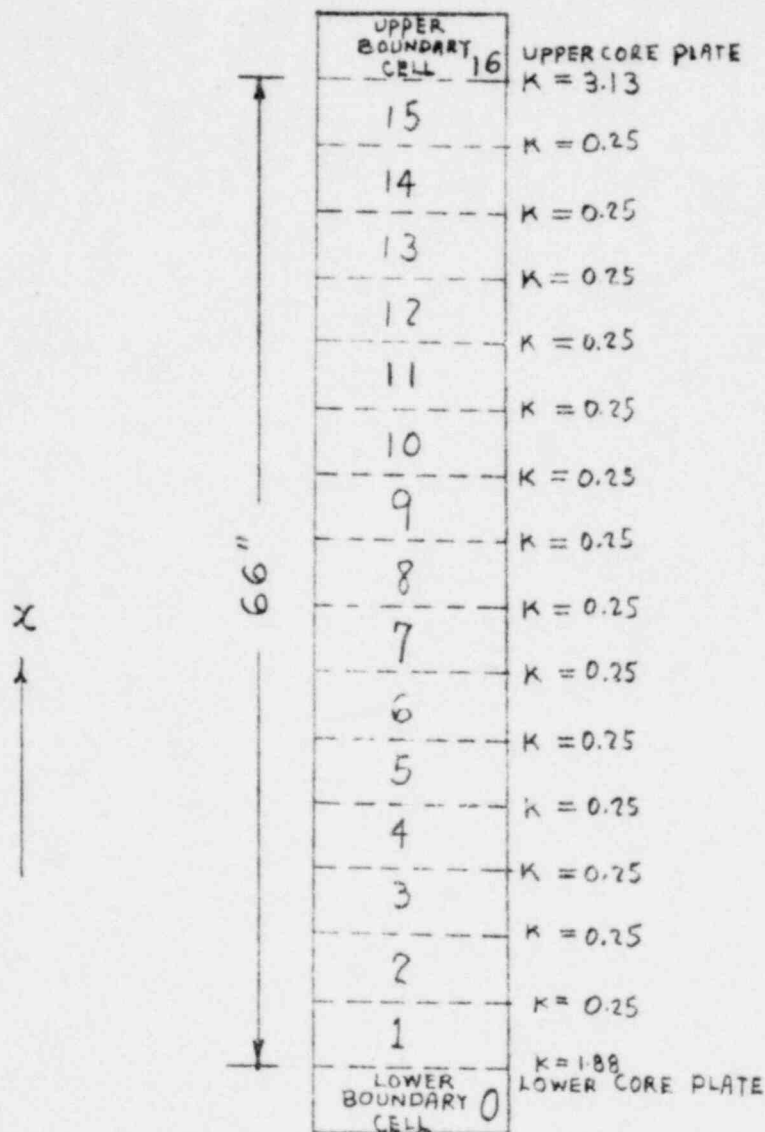


FIG. 2. FUEL ROD ASSEMBLY AXIAL CELL ARRANGEMENT FOR MOXY/SCORE MODEL

III. ANALYSIS APPROACH

In this section, the method by which spatial nonuniform coolant mass flow conditions were modeled in the MOXY/SCORE calculations will be discussed. The first approach considered was to apply nonuniformities directly to the boundary conditions. The second approach considered was to extend the computational grid into the upper plenum, which would calculate any possible nonuniformities. In considering this approach to performing the analysis, the geometrical complexities of the upper plenum were found to make specifying an unequivocally uniform upper boundary condition quite dubious - furthermore, the many changes in area and flow direction would have been difficult to model. Finally, a larger computational grid would have increased the expense of the analysis. Constraints on time and uncertainty in modeling the complex fluid behavior in the upper plenum regions led to the decision to not use this approach. The approach chosen was to apply the nonuniformities to the boundary conditions. The means by which this was accomplished is discussed.

Because spatial nonuniformity was the parameter of interest, the problem was constrained by the conditions of maintaining the temporal dependence of total mass flow rate across the upper and lower boundaries as nearly equal to that of the base case as possible. Limitations on boundary conditions that can be used in a MOXY/SCORE calculation made it impossible to meet this constraint while changing the spatial dependence of mass flux at the upper boundary. However, these conditions could be met at the lower boundary. (The reader is referred to Appendix A for a detailed discussion of this topic.)

Since the basic concern about the effect of spatially nonuniform boundary conditions was whether it would have significant effect on calculated fuel rod temperatures at the hot axial level, it was judged that nonuniformities at the bottom boundary would have as much effect

on fuel rod temperatures at the hot axial level as would nonuniformities at the top boundary. Therefore, to minimize time and expense in the analysis, spatial nonuniformities were applied to the boundary conditions at the bottom of the core during downflow. Otherwise, the boundary conditions were the same as for the base case.

Below is defined the method for specifying the variation of axial velocity distribution (which will result in the variation of coolant mass flux.)

If one defines: (core inlet = the bottom of the core)

$v_i(t)$ = unperturbed (base case) inlet axial velocity in the i -th flow channel at time t , and

$v_i'(t)$ = perturbed inlet axial velocity in the i -th flow channel at time t .

Then the unperturbed total volume rate will be equal to the perturbed total volume rate at the bottom of the core if

$$\sum_{i=1}^{16} v_i(t) = \sum_{i=1}^{16} v_i'(t) \quad (3-1)$$

The equality between unperturbed and perturbed total volume rates does not generally imply the equality between unperturbed and perturbed total mass rate. However, for the current calculations, the density across the bottom core boundary is essentially flat, so the equal volume rate condition implies constant total mass rate at the bottom of the core. (The results of MOXY/SCORE calculations vindicate this assumption.) In other words, Equation (3-1) is the condition that the temporal dependence of total mass rate will not be varied.

998 011

Because unperturbed inlet axial velocities are spatially independent, Equation (3-1) can be rewritten as:

$$\sum_{i=1}^{16} v_i'(t) = 16 \bar{v}(t) \quad (3-2)$$

with $v(t) = v_i(t)$ for $i=1, \dots, 16$. Equation (3-2) is the basic constraint condition for axial velocity perturbation.

If y_i and z_i denote coordinates of channel no. i (see Figures 1 and 3), the distance between channel no. i and channel no. 1 is $\sqrt{y_i^2 + z_i^2}$. To specify the shape of the perturbed axial velocity distribution, it is assumed that $(v_i'(t) - v_1'(t))$ will be proportional to $\sqrt{y_i^2 + z_i^2}$. This assumption coupled with Equation (3-2) implies that (see Appendix B)

$$x_i(t) = (1 - 0.416 \sqrt{y_i^2 + z_i^2}) x_1(t) + 0.416 \sqrt{y_i^2 + z_i^2}, \quad i=1,2,\dots,16, \quad (3-3)$$

with

$$x_i(t) = \frac{v_i'(t)}{\bar{v}(t)} \quad i = 1,2,\dots,16. \quad (3-4)$$

According to Equation (3-3), the inlet axial velocity perturbation is completely specified if $x_1(t)$ is given. If $x_1(t) = 1$, Equation (3-3) implies that $x_i(t) = 1$ for $i=1,2,\dots,16$, i.e., there is no perturbation. With reasons given previously, it will be assumed that $x_i(t)=1$ when flow is in the normal direction at the core inlet. According to Figure 4, flow reverses when $0.339 \text{ sec} < t < 2.673 \text{ sec}$ or $t > 11.536 \text{ sec}$. Three MOXY/SCORE calculations (which will be designated as Run #2, Run #3, and Run #4 respectively) were carried out and were characterized by:

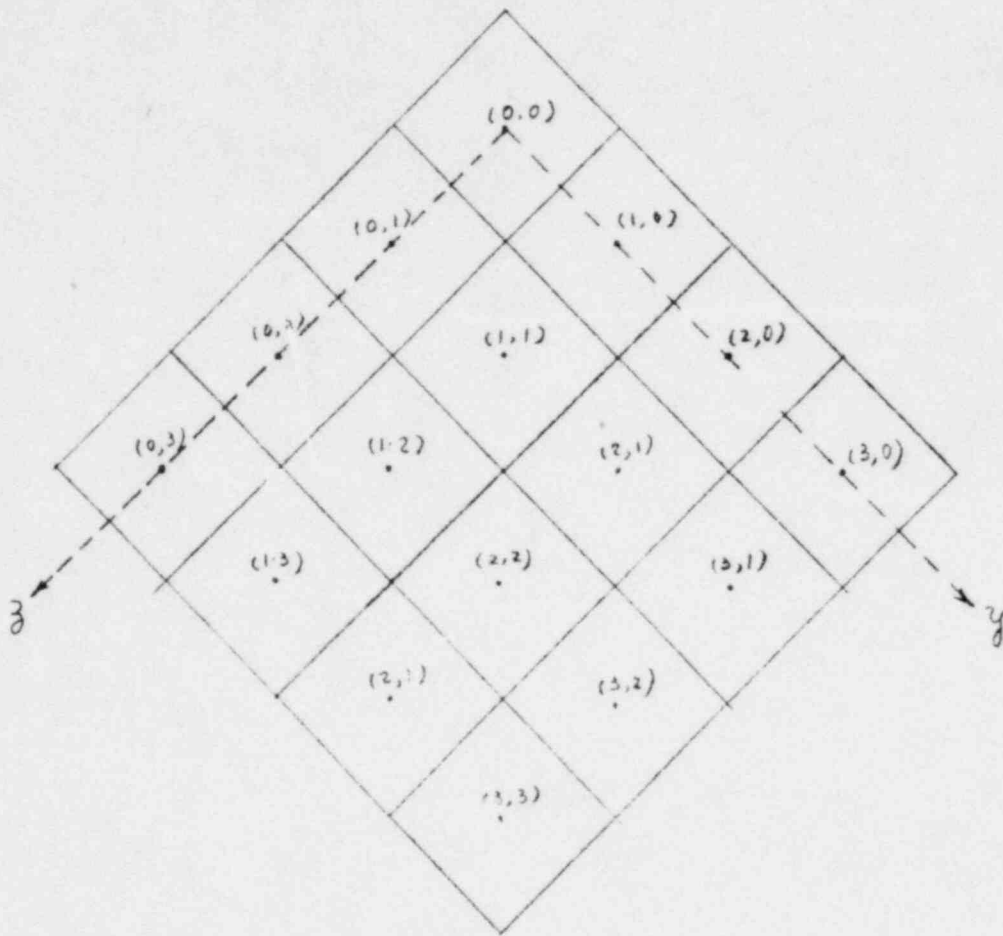


FIG. 3. FLOW CHANNEL COORDINATES

898 013

————— RUN # 1 (FOR ALL INLET BOUNDARY CELLS)

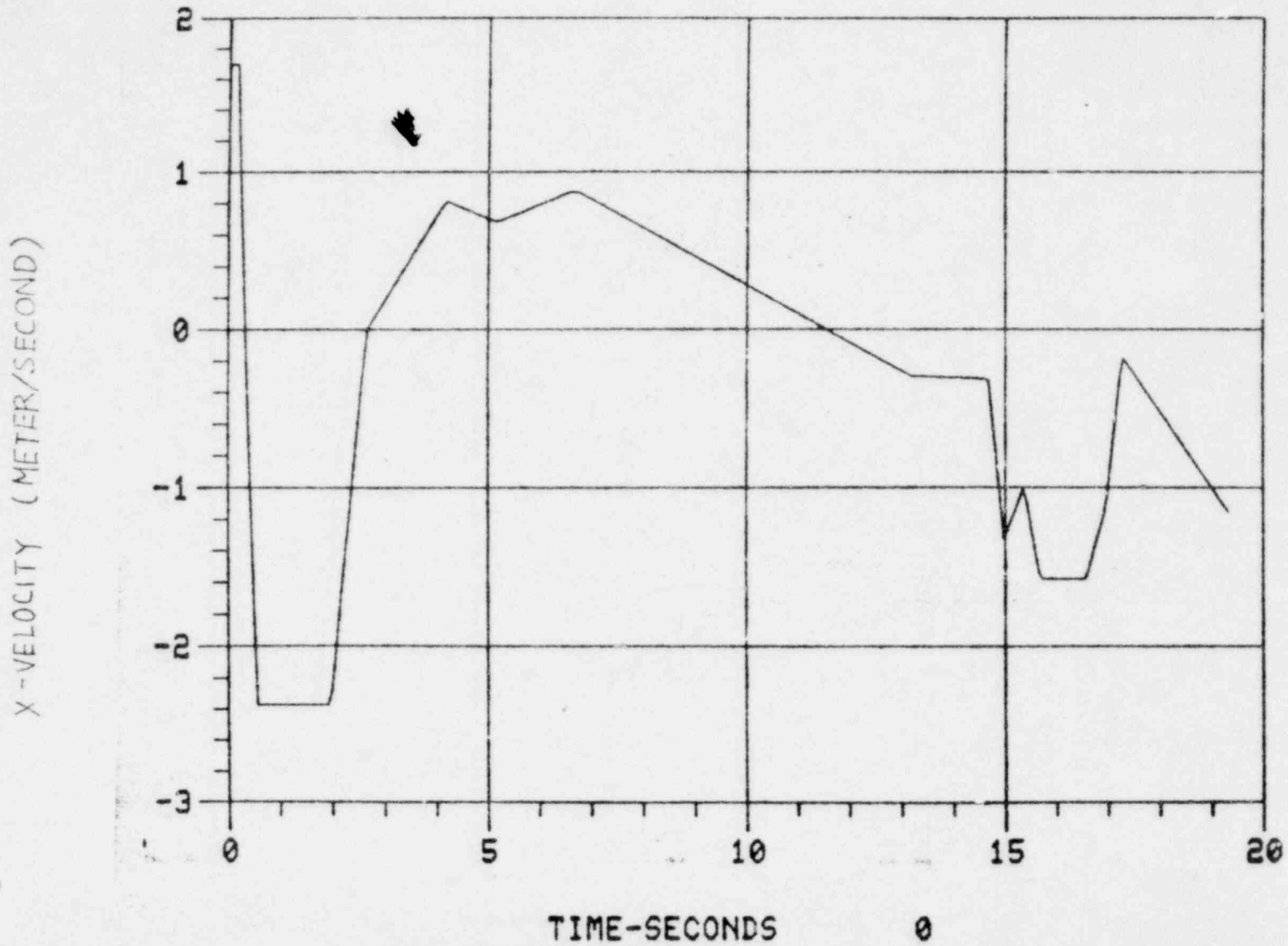


FIG. 4. INLET BOUNDARY CELL AXIAL VELOCITY (RUN # 1)

- (a) Run #2: $x_1(t) = 1.2$ for $0.339 \text{ sec.} < t < 2.673 \text{ sec.}$ and $t > 11.536 \text{ sec.}$
- (b) Run #3: $x_1(t) = 1.6$ for $0.339 \text{ sec.} < t < 2.673 \text{ sec.}$ and $t > 11.536 \text{ sec.}$
- (c) Run #4: $x_1(t) = 1.6$ for $0.339 \text{ sec.} < t < 2.673$ and $x_1(t) = 2.0$ for $t > 11.536 \text{ sec.}$

Except for the inlet axial velocity distribution, all input data for Runs #2, #3, and #4 are identical to Run #1 (the values of $x_i(t)$ ($i=1, 2 \dots, 16$) as given by Equation (3-3) for $x_1(t) = 1.2, 1.6$ and 2.0 are shown in Figures 20, 21 and 22, respectively).

The results of Run #2, Run #3, and Run #4 will be compared with those of Run #1 in next section. The comparisons will show that the effect of nonuniform boundary flow distribution on peak cladding temperature is very small. As a matter of fact, the effect is so small that it is expected the effect will still be negligible even if $x_1(t)$ is much larger than those assigned to current calculations. It is due to this observation that no calculation with higher value of $x_1(t)$ was performed.

998 015

IV. RESULTS AND ANALYSIS

The comparison and evaluation of Run #1, Run #2, Run #3 and Run #4 will be given in this section. The notation established in Item (c) of Section 2 will be used throughout.

It was found that the differences between the results of the MOXY/SCORE calculations are generally small. Because Run #4 represents the largest perturbation compared with Run #1 (the base case), only the results of Run #1 and Run #4 will be presented and compared. The presentation will be further limited to thermal-hydraulic properties related to flow Channel No. 1, since the peak cladding temperature occurs in that channel.

Figures 5, 6, 7, and 8 depict axial velocities at FC 1-0, FC 1-1, FC 1-2 and FC 1-3 for Run #1 and Run #4. It is seen that the effect of the inlet axial velocity perturbation is limited to the first few axial levels. Figure 9 depicts Y-velocities at FC 1-1 for Run #1 and Run #4. (The crossflow resistance correlations are given in Table A-I and A-II of Reference 3. For this study, Model Option is "0".) Inlet axial velocity perturbations apparently cause a sharp increase of crossflow which, in turn, leads to a rapid resoration of the original (unperturbed) axial velocity distribution at higher axial levels.

The implication of this phenomenon is that the axial velocity perturbation at the core inlet will not have a strong effect on the LOFT core bulk thermal-hydraulic behavior.

Figures 10-19 provides the comparisons (between Run #1 and Run #4) of several thermal-hydraulic parameters at FC 1-9 (where the peak cladding temperature occurs). These parameters are:

- (1) Axial velocity
- (2) Fluid quality

998 016

— RUN # 1 (FC 1-0)
- - - RUN # 4 (FC 1-0)

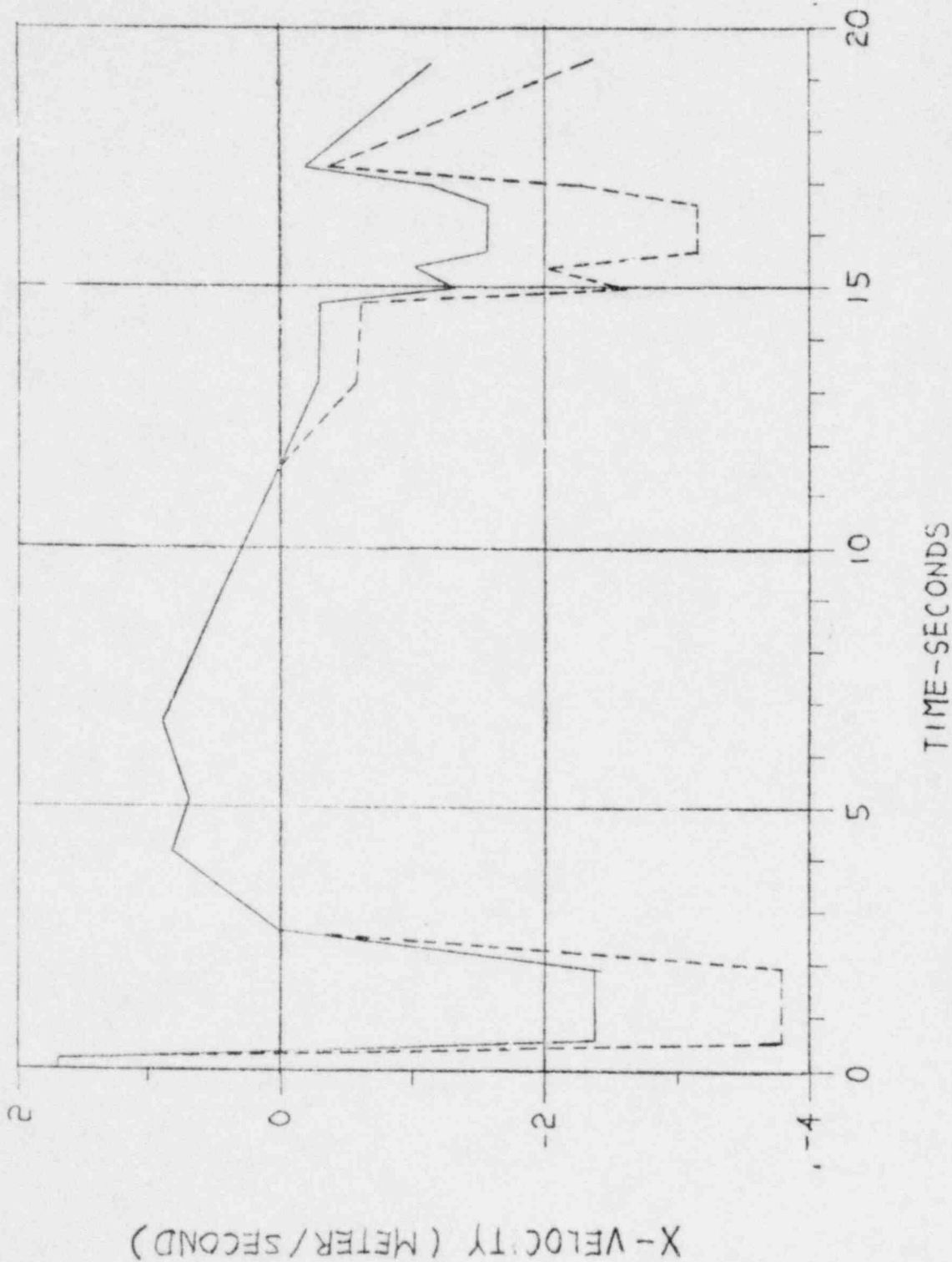


FIG. 5 . COMPARISON OF X-VELOCITIES AT THE CORE INLET

896 017

X-VELOCITY (METER/SECOND)

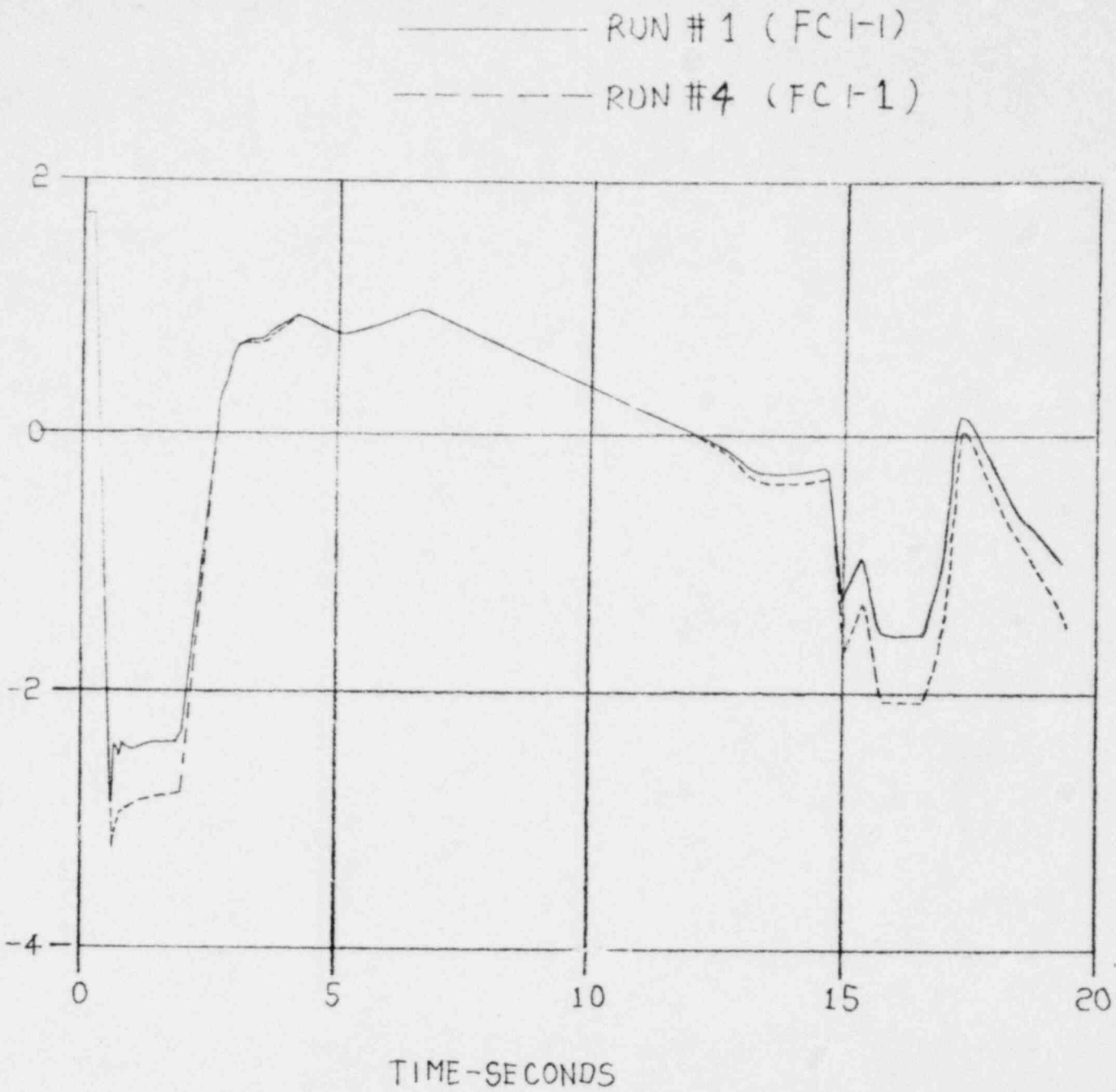


FIG. 6. COMPARISON OF X-VELOCITIES AT FIRST AXIAL LEVEL

16

119 866

X-VELOCITY (METER/SECOND)

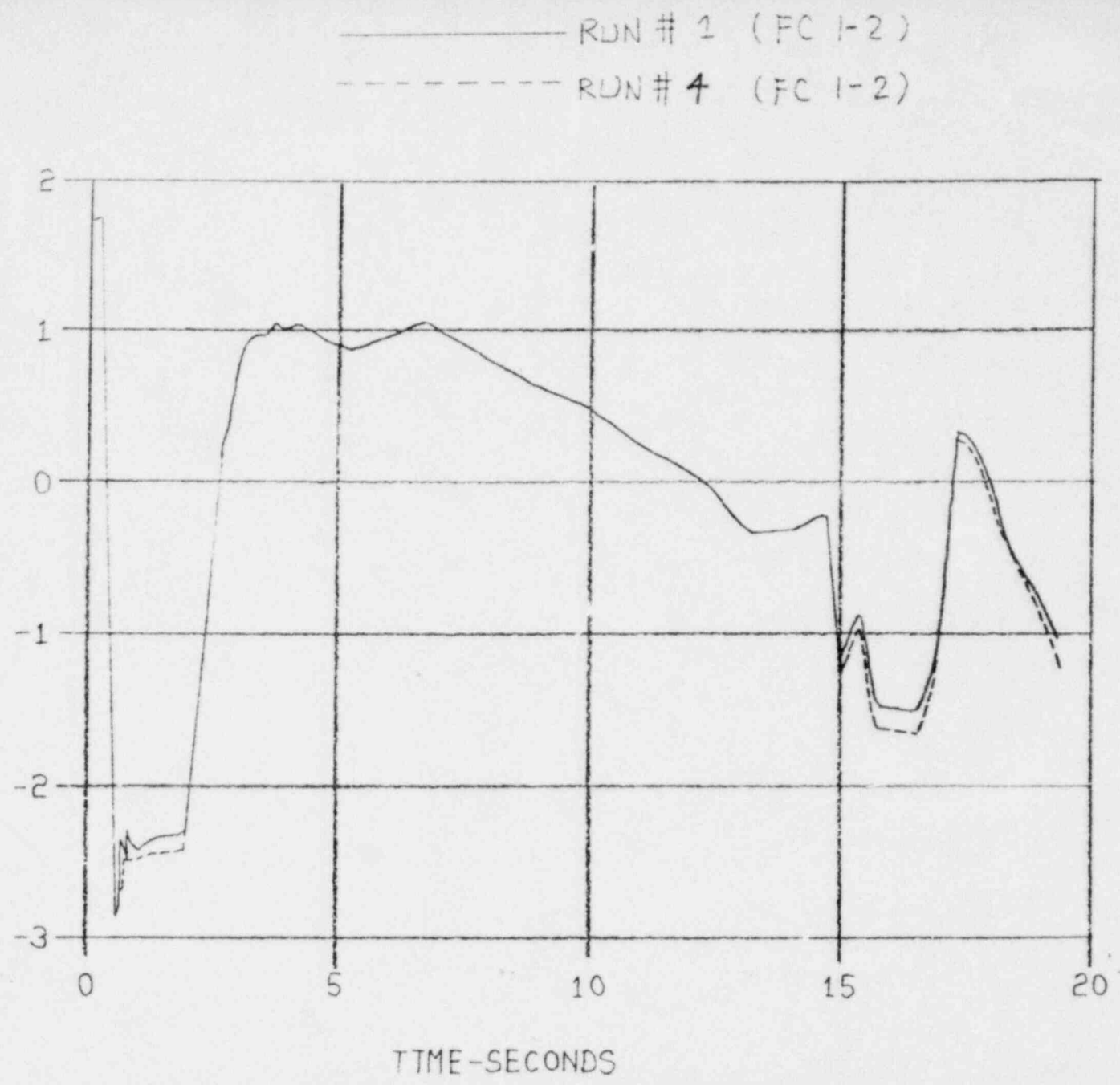
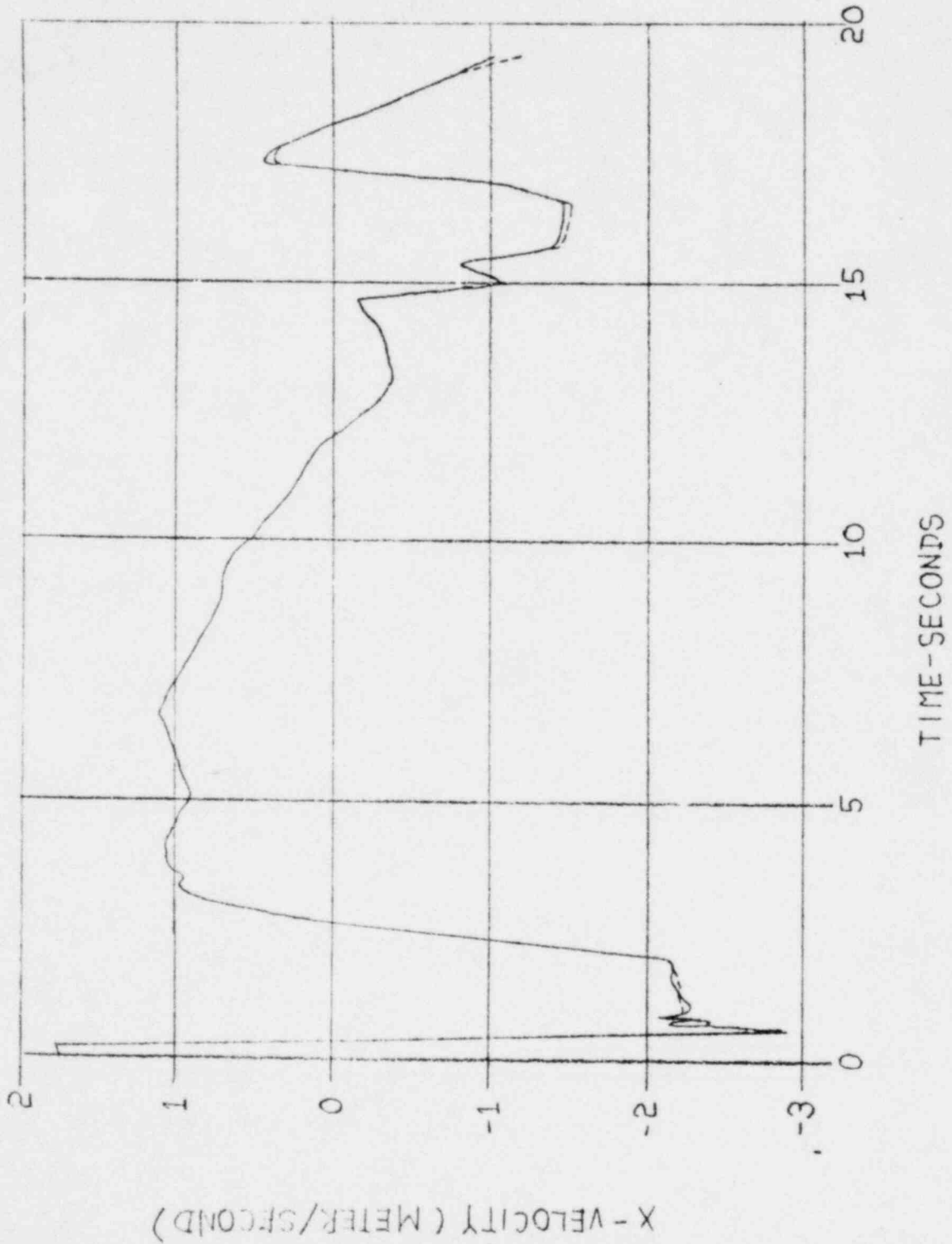


FIG. 7. COMPARISON OF X-VELOCITIES AT SECOND AXIAL LEVEL

LIR 1111-01

— RUN #1 (FC 1-3)
- - - RUN #4 (FC 1-3)



020 866

FIG. 8. COMPARISON OF X-VELOCITIES AT THIRD AXIAL LEVEL

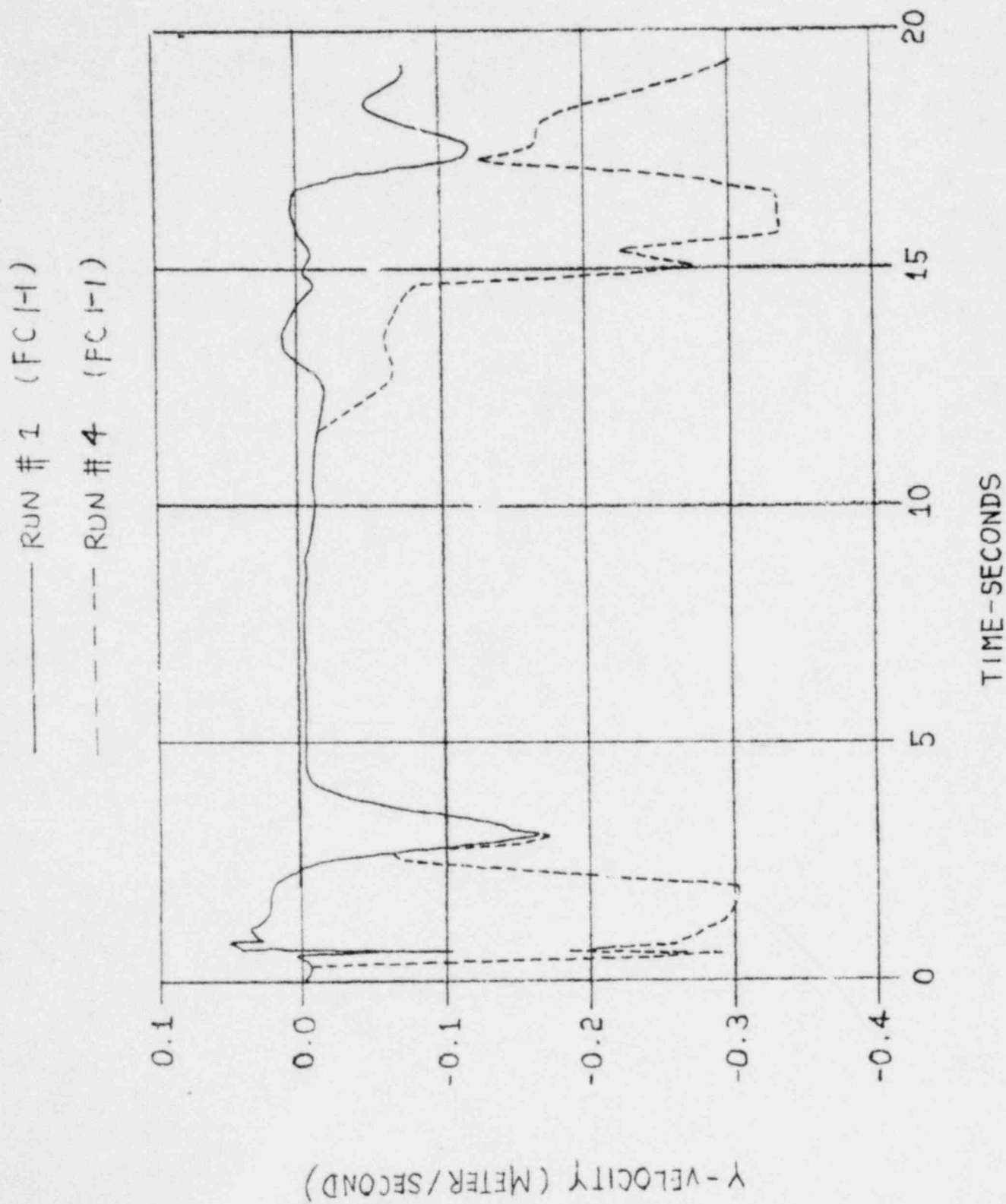


FIG. 9. COMPARISON OF Y-VELOCITIES AT FIRST AXIAL LEVEL

120 866 021

— RUN #1 (FC 1-9)
- - - RUN #4 (FC 1-9)

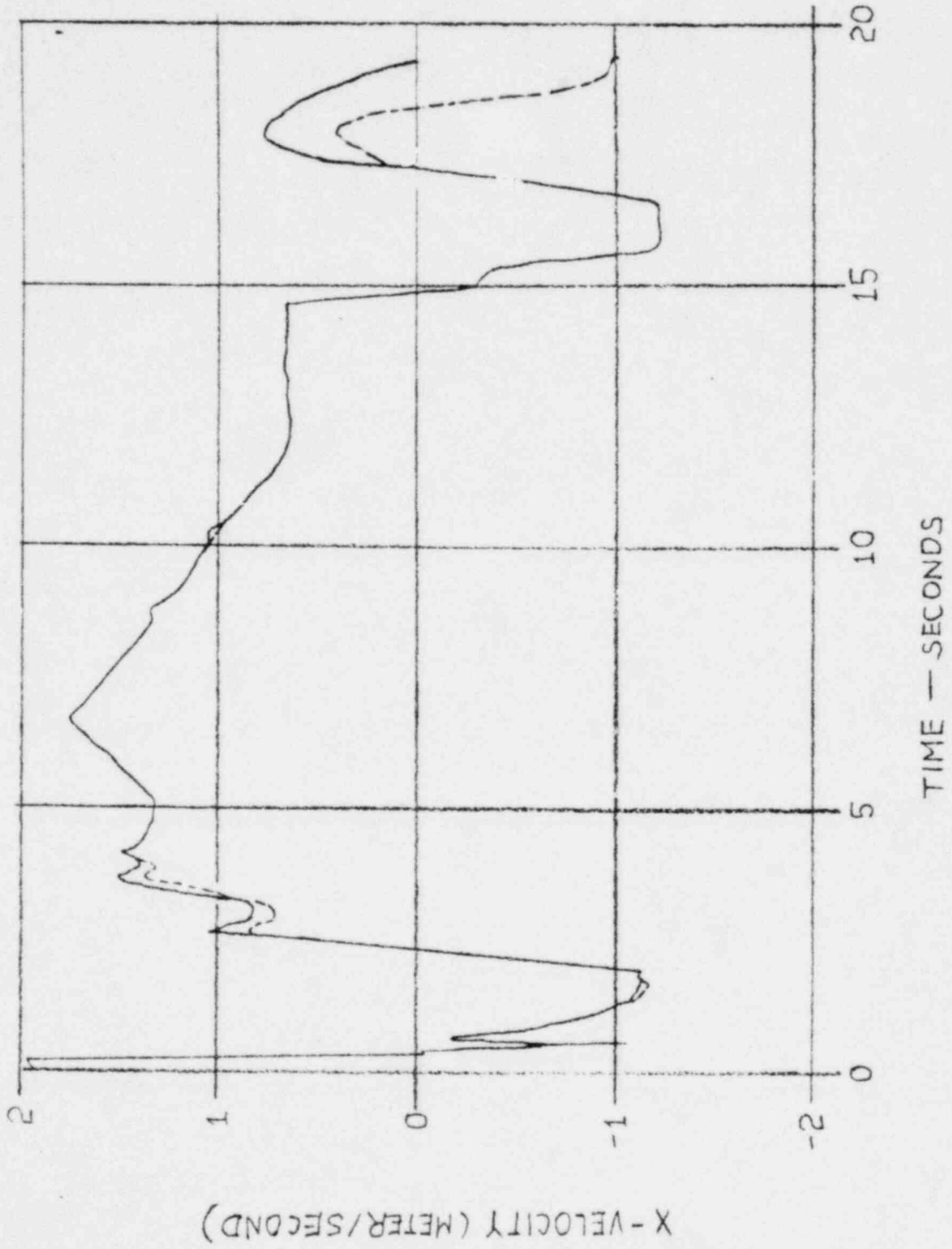


FIG.10. COMPARISON OF X-VELOCITIES AT NINTH AXIAL LEVEL

220 866

— RUN #1 (FCI-9)
- - - RUN #4 (FCI-9)

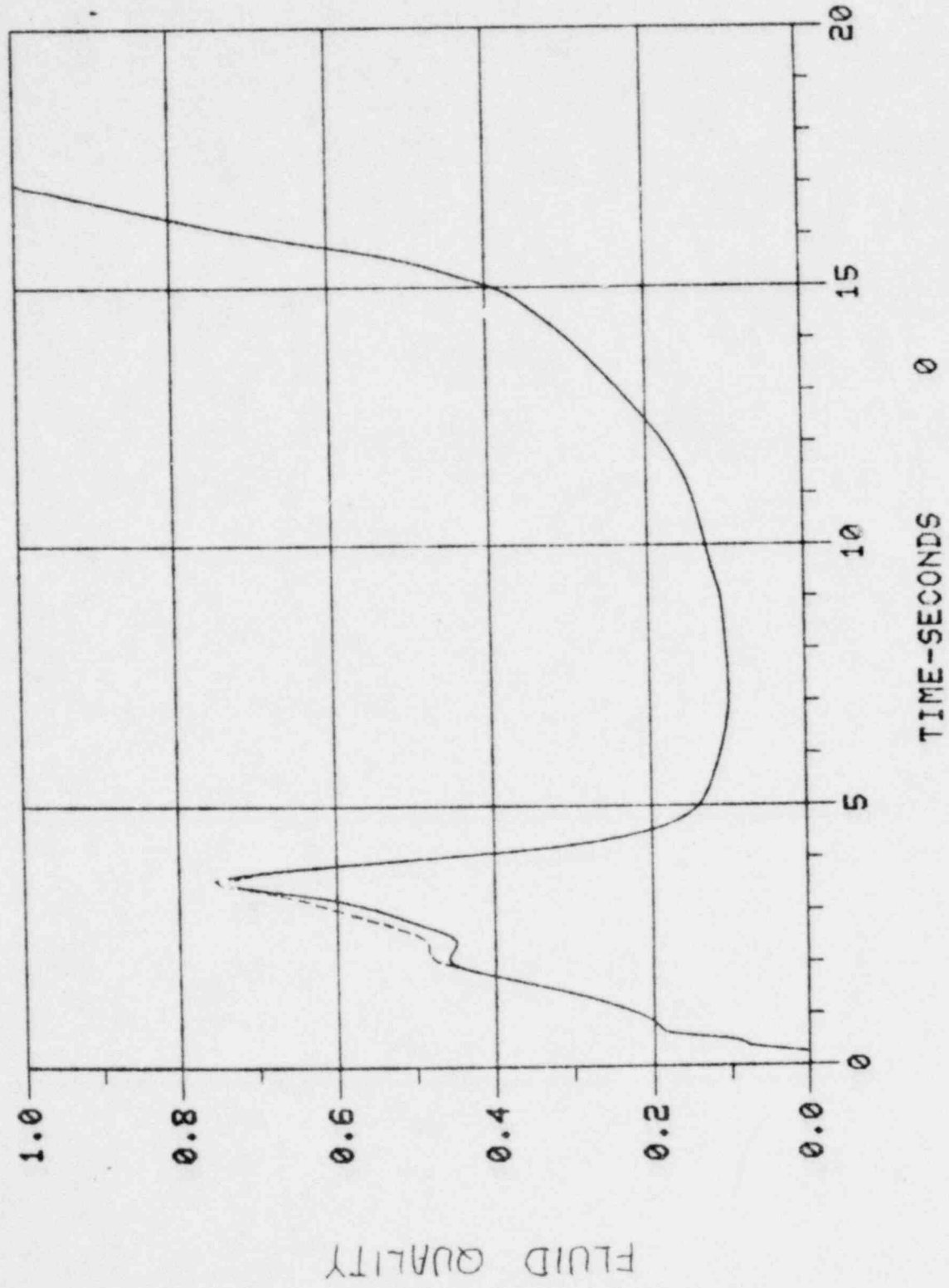


FIG. 11. COMPARISON OF FLUID QUALITIES AT NINTH AXIAL LEVEL

898 023

— RUN #1 (FC 1-9)
- - - RUN #4 (FC 1-9)

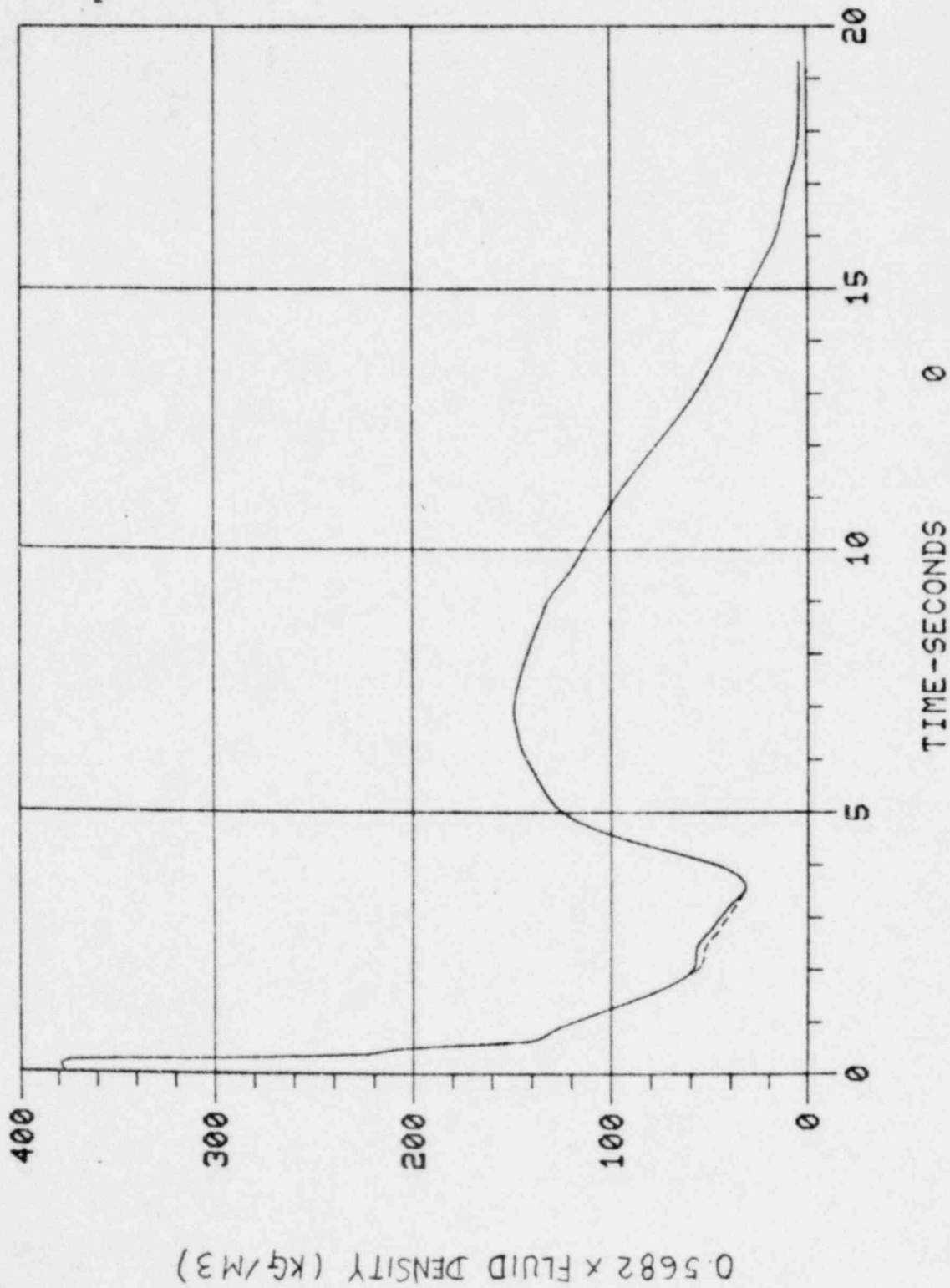


FIG. 12. COMPARISON OF FLUID DENSITIES AT NINTH AXIAL LEVEL

865 024

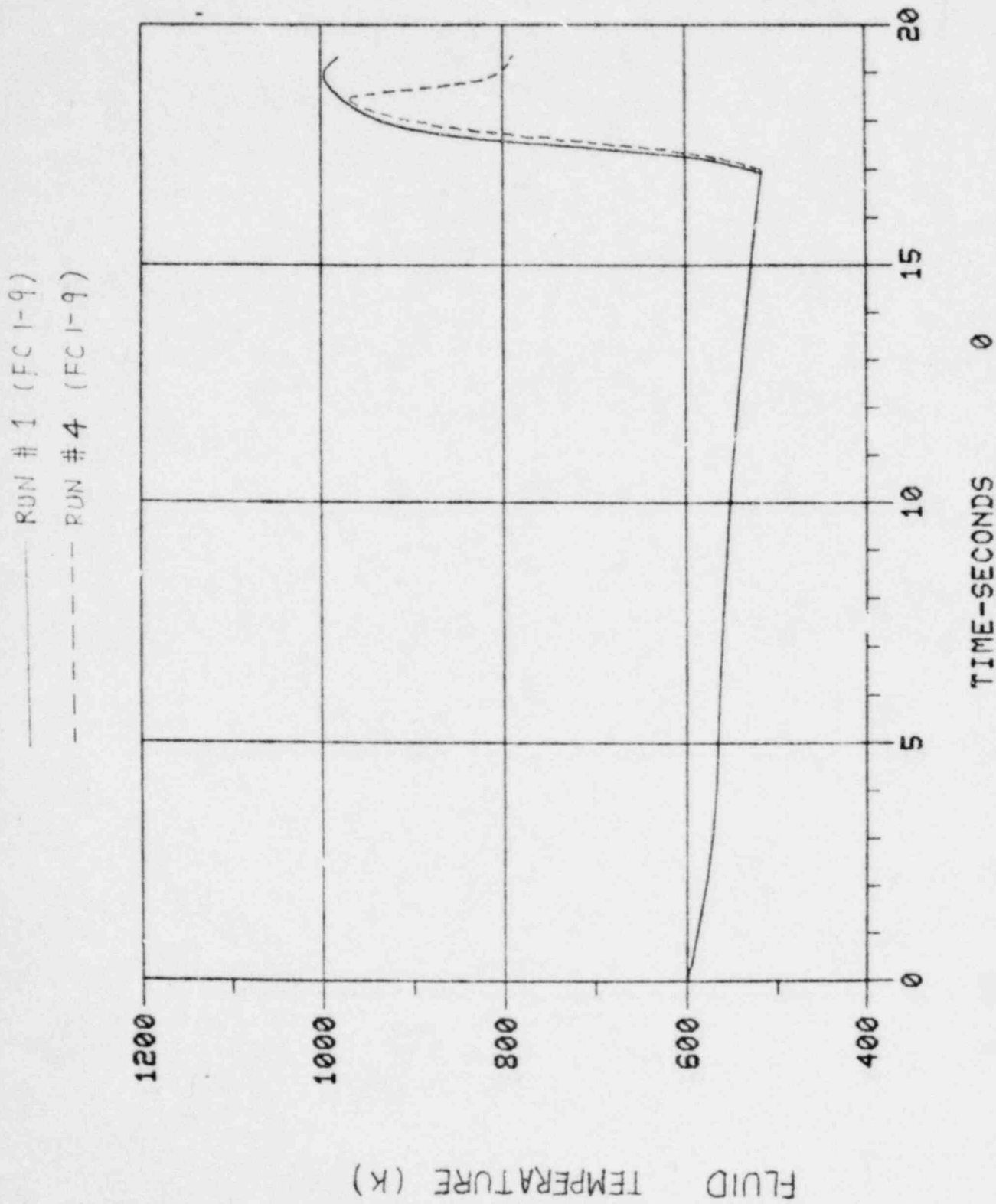


FIG. 13. COMPARISON OF FLUID TEMPERATURES AT NINTH AXIAL LEVEL

998 026

FLUID PRESSURE (N/M²)

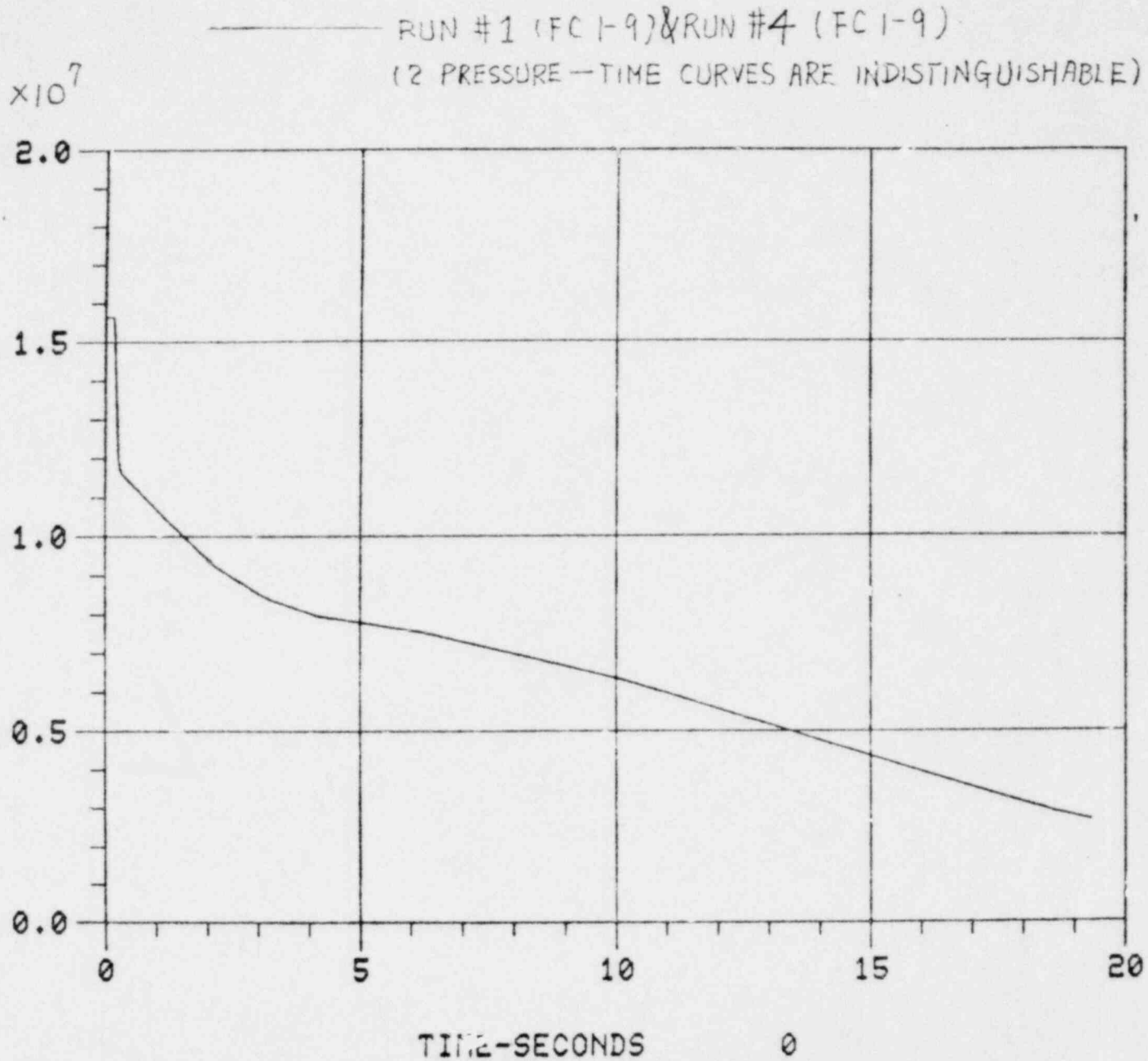
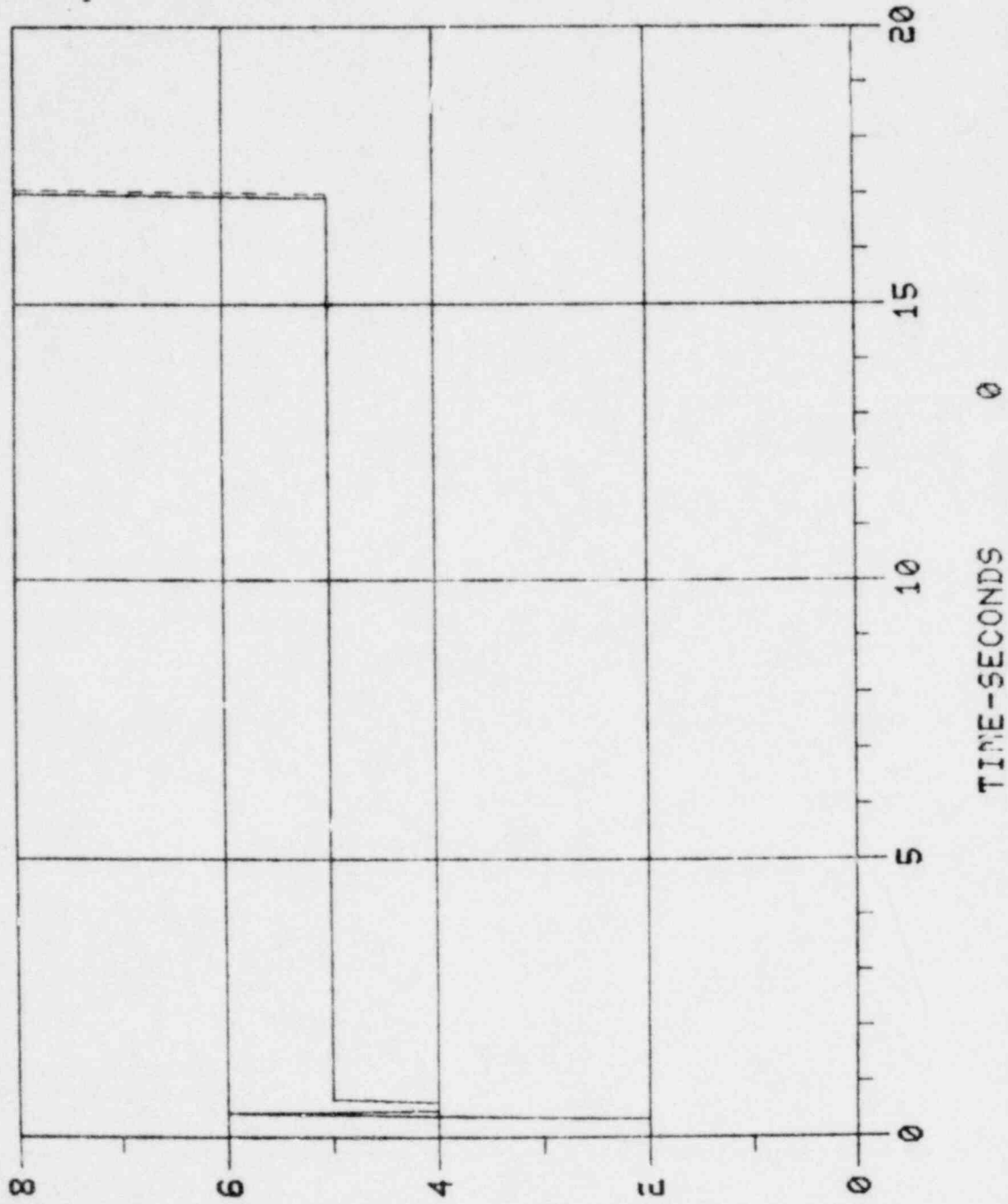


FIG. 14 COMPARISON OF FLUID PRESSURES AT NINTH AXIAL LEVEL

— RUN #1 (FRHS I-9)
- - - RUN #4 (FRHS I-9)



CONVECTIVE HEAT TRANSFER MODE

FIG. 15. COMPARISON OF HEAT TRANSFER MODES AT NINTH AXIAL LEVEL

868 021

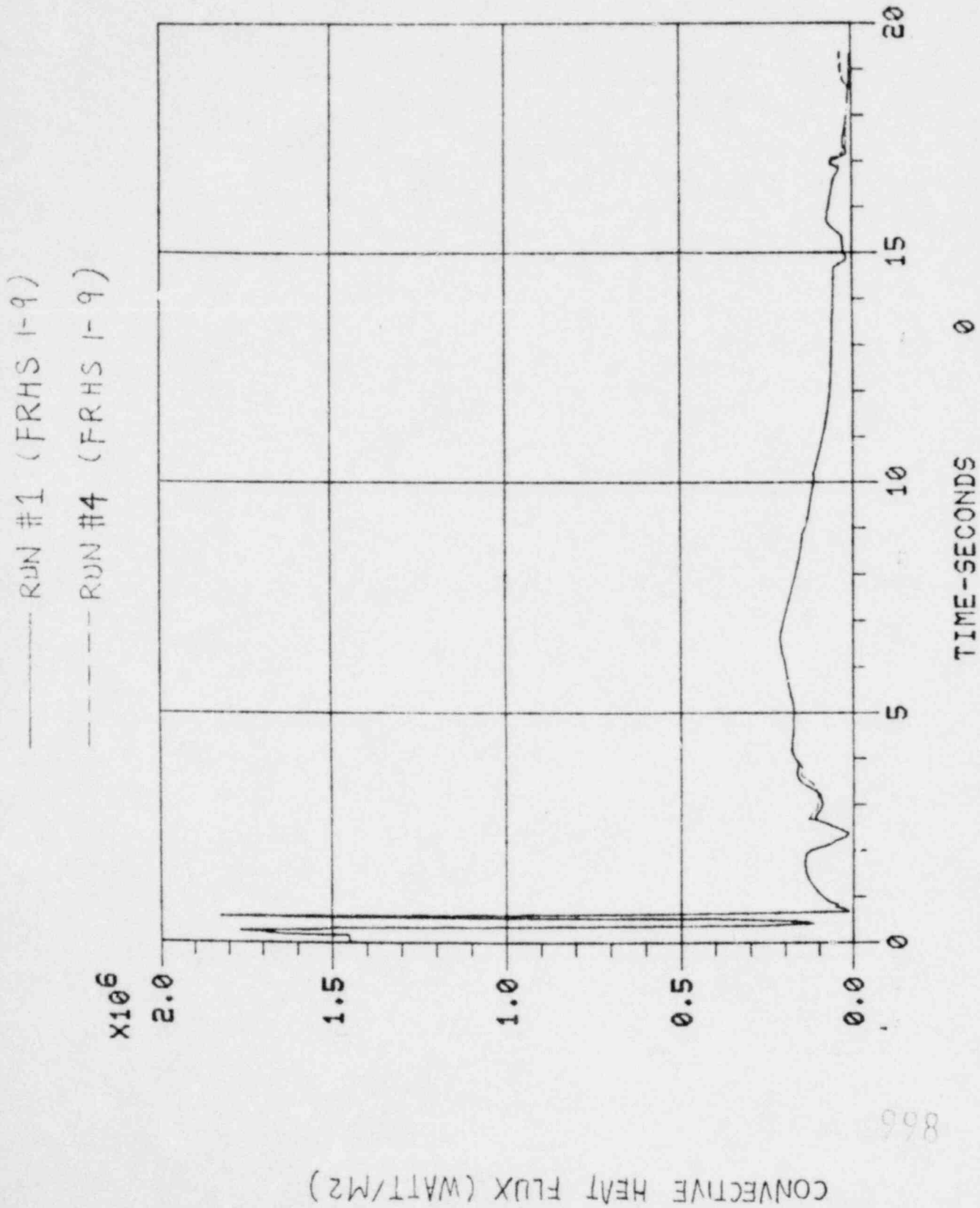


FIG 16. COMPARISON OF CONVECTIVE HEAT FLUXES AT NINTH AXIAL LEVEL

898-020

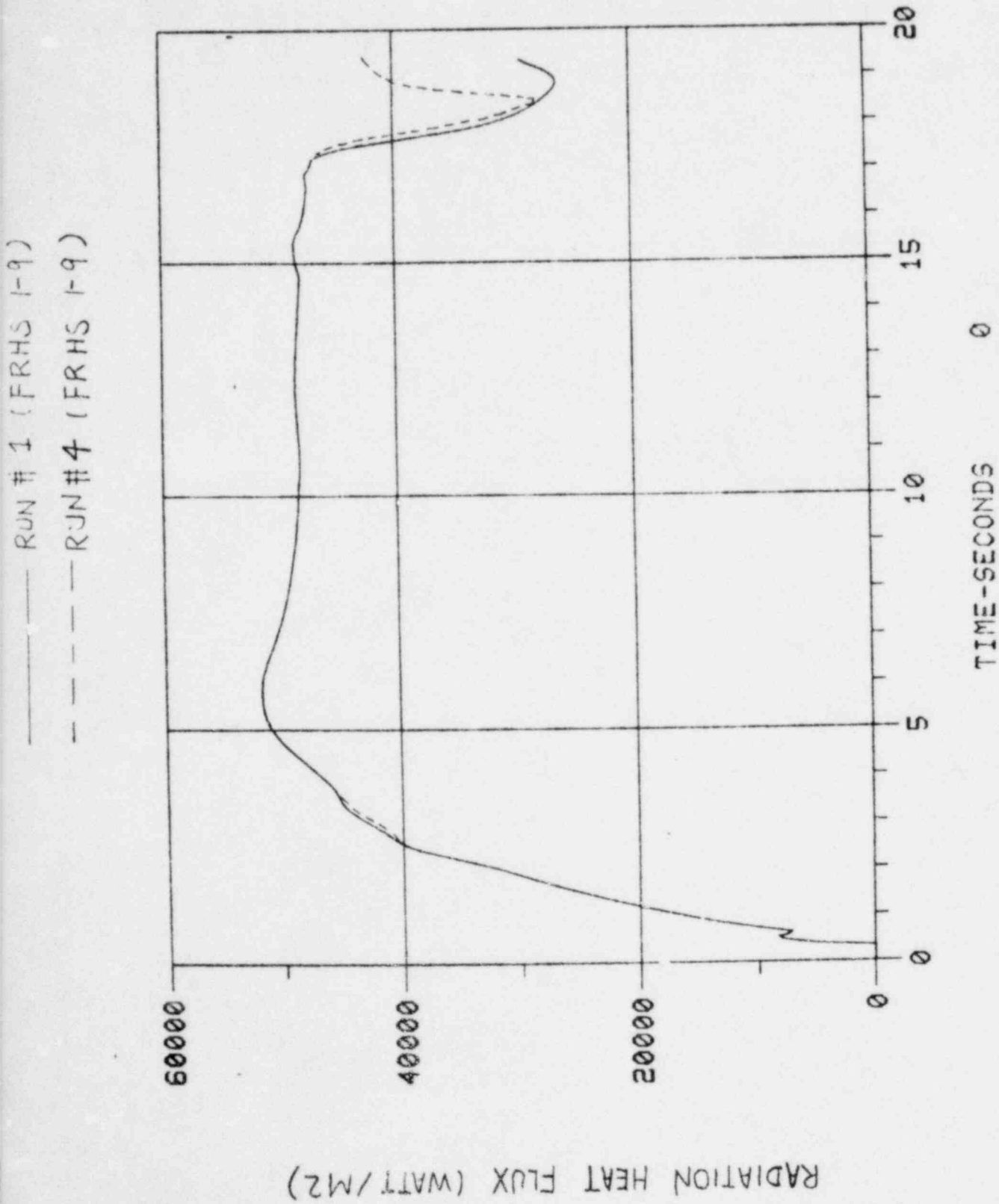


FIG. 17. COMPARISON OF RADIATION HEAT FLUXES AT NINTH AXIAL LEVEL

998 029

— RUN # 1 (FRHS 1-9)
- - - RUN # 4 (FRHS 1-9)

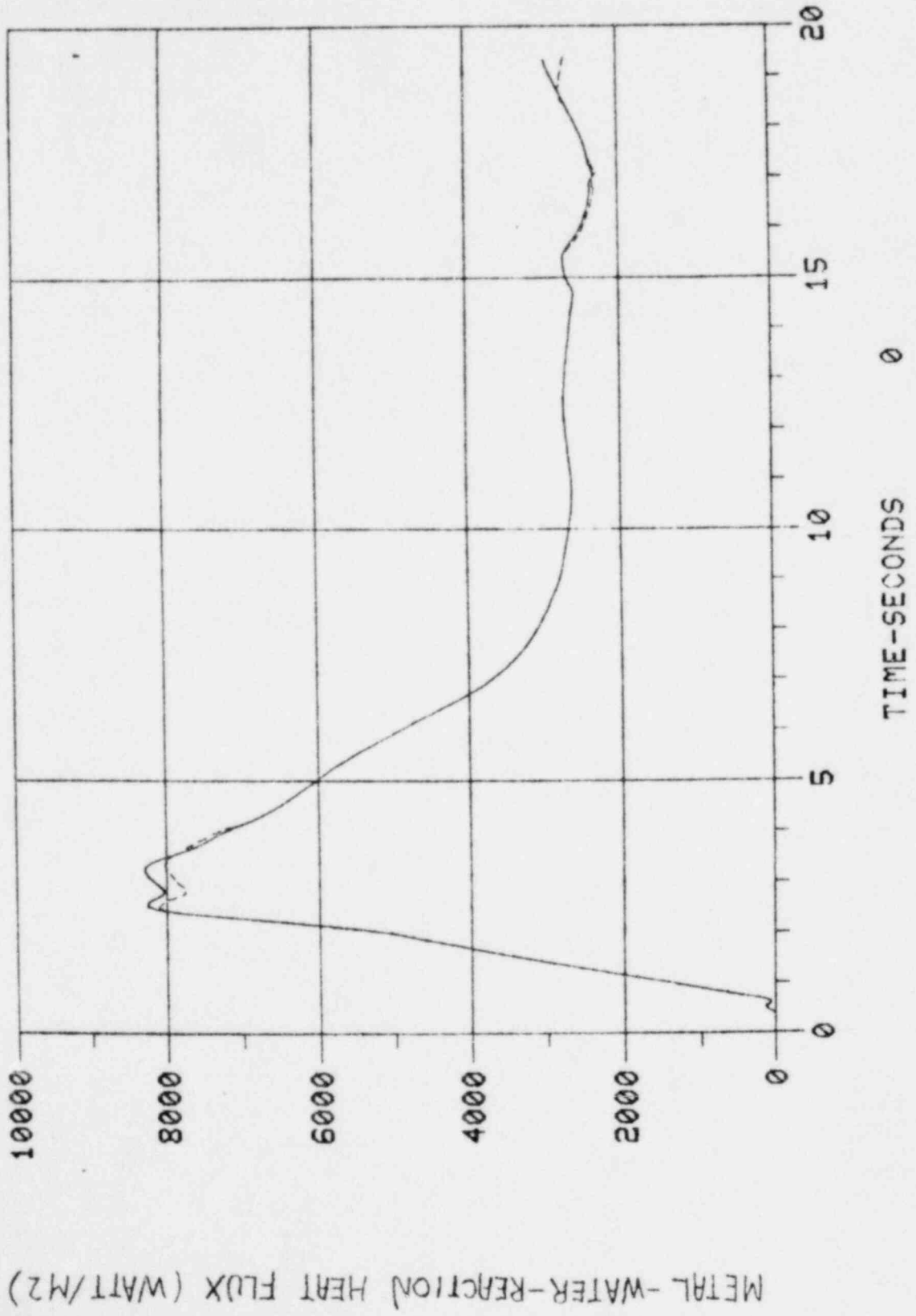
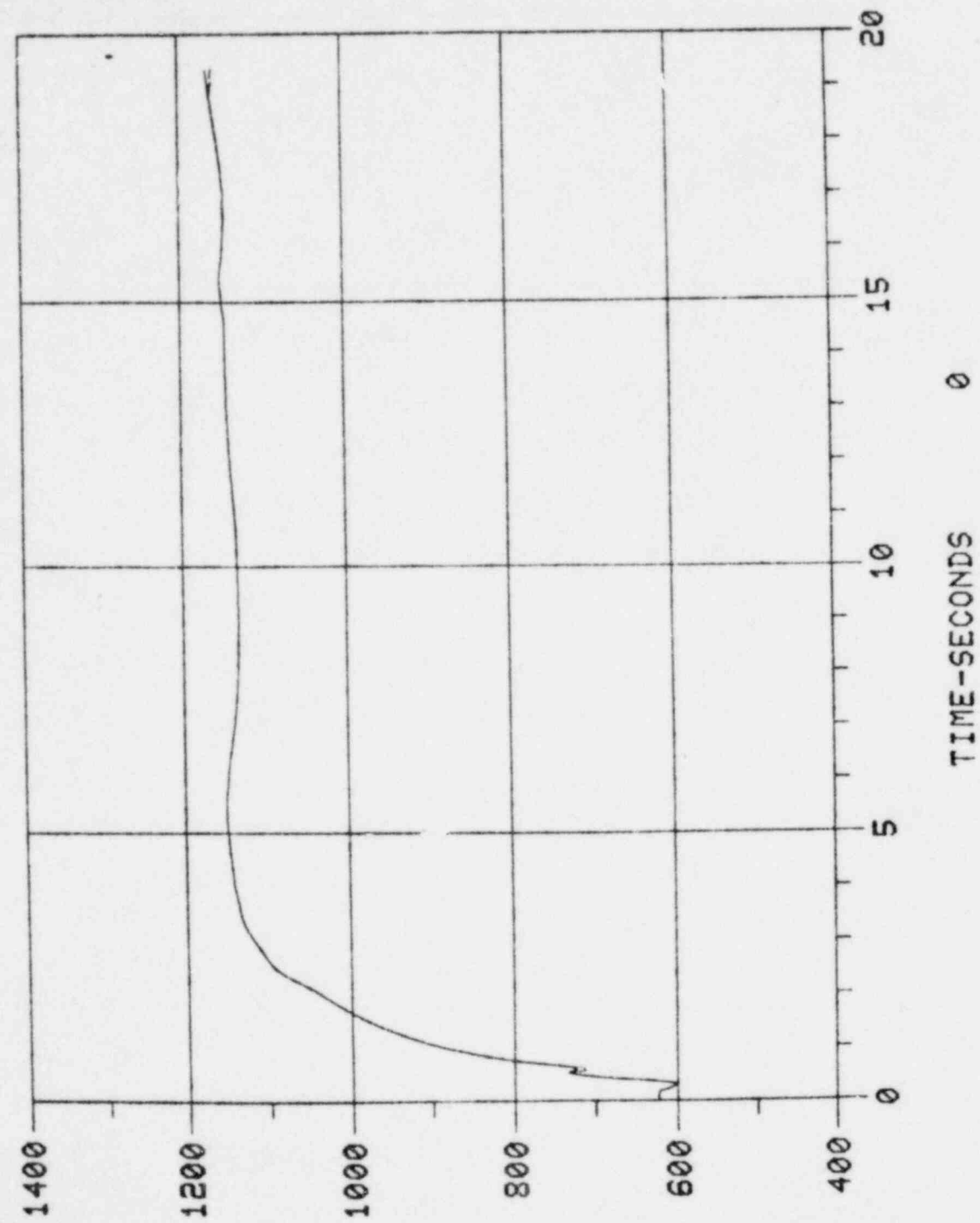


FIG. 18. COMPARISON OF METAL-WATER-REACTION HEAT FLUXES AT NINTH AXIAL LEVEL

METAL-WATER-REACTION HEAT FLUX (WATT/M²)

998 030

— RUN #1 (FRHS 1-9)
- - - RUN #4 (FRHS 1-9)



CLADDING OUTSIDE SURFACE TEMPERATURE (K)

FIG. 19. COMPARISON OF CLADDING TEMPERATURES AT NINTH AXIAL LEVEL

866 031

- (3) Fluid density
- (4) Fluid temperature
- (5) Fluid pressure
- (6) Convective heat transfer mode
- (7) Convective heat flux
- (8) Radiation heat flux
- (9) Metal-Water-Reaction heat flux
- (10) Cladding outside surface temperature.

The comparisons given in Figures 10-19 indicate that the effects of inlet axial velocity perturbations become appreciable only after coolant becomes superheated (at $t=17$ seconds). It should be noted, however, that Equation (3-1) will no longer guarantee that the given temporal dependence of total mass rate will be maintained after the vapor fraction at the bottom of the core becomes high. In other words, after $t=17$ seconds, one might have seen the effects of the variation of the temporal dependence of total mass rate rather than these of mass flux distribution at the bottom of the core.

V. CONCLUSIONS AND RECOMMENDATIONS

A preliminary study of the consequences of axial velocity perturbation at the bottom of the core has been completed. The principle conclusions of this study are:

- (1) The effect of the flow nonuniformity at the bottom of the core is neutralized by a strong flow redistribution in the lower two or three axial levels (the entire core is divided into 15 axial levels). The implication is that the flow nonuniformity at the bottom of the core has no significant effect on the thermal-hydraulic behavior (includes cladding temperature) at the hot plane. Because the degree of flow nonuniformity specified in MOXY/SCORE calculations is rather large, this conclusion should be valid even if actual condition of flow nonuniformity is applied.
- (2) The cause behind the large flow redistribution mentioned in (1) is likely to be the large radial gradient of core power distribution. If it is indeed the case, a large flow redistribution will also neutralize the effect of the flow nonuniformity at the top of the core.

This study represents a first attempt toward the understanding of the hypothesized phenomenon of selective cooling due to nonuniform flow at the core boundaries. If a more thorough study on this phenomenon is needed, it is recommended that:

- (1) The computer program TRAC be used to carry out a 3-D thermal-hydraulic analysis of the entire LOFT reactor vessel under LOCA conditions. At the vessel fluid boundaries, uniform fluid conditions will be specified.

998-035

- (2) TRAC also be used to carry out a corresponding 1-D calculation with the identical boundary conditions. The comparison between the results of these two calculations should provide a better understanding toward the effects of nonuniform flow at the core boundaries.

APPENDIX A

BOUNDARY CONDITION SPECIFICATIONS

998-035

APPENDIX A

BOUNDARY CONDITION SPECIFICATIONS

As a prerequisite to any MOXY/SCORE calculation, the user must specify, at the core boundary, the temporal and spatial dependence of certain thermal-hydraulic parameters. According to Table B-I of Reference 3, these parameters are fluid axial velocity, pressure and internal energy. A further restriction is that fluid axial velocity and pressure cannot be specified at the same boundary (otherwise one would have a set of mathematically inconsistent boundary conditions). As a result of these constraints, the user can specify the boundary conditions only in the following combinations:

- (a) fluid axial velocity and internal energy at one core boundary; pressure and internal energy at the other,
- (b) pressure and internal energy at both core boundaries,
- (c) velocity and internal energy at both core boundaries.

Among these combinations, both (b) and (c) have a serious drawback. If one specifies boundary conditions according to (b) and (c), generally, the thermal-hydraulic conditions within the reactor core will vary substantially if a slight change in boundary conditions occurs. In other words, a slight error in the specification of boundary conditions might mean a large error in the results of the calculation. This drawback is easy to understand for (b). Generally, the system pressures at the top and the bottom of the core are much larger than the pressure drop within the core (the ratio is in the order of 1000:1). A slight error in the specification of system pressures at the core boundaries obviously will cause a large error of the pressure drop within the core and thus generate a large shift of thermal-hydraulic conditions within the core.

Because one does not have absolute confidence on the accuracy of the given boundary conditions, (a) is picked over (b) and (c). One further decides that fluid axial velocity should be specified at the bottom of the core because the assumption of uniform axial velocity distribution is valid there.

The MOXY/SCORE computer program does not allow the specification of the temporal and spatial dependence of fluid density at core boundaries. As a result, the temporal dependence of total mass rate at a core boundary cannot be specified. It is completely determined by other boundary conditions and internal thermal-hydraulic calculations.

998 037

APPENDIX B

BOUNDARY AXIAL VELOCITY DISTRIBUTION

The derivation of equation (3-3) is given in this appendix.

First one assumes that $(v_i'(t) - v_i(t))$ will be proportional to

$\sqrt{y_i^2 + z_i^2}$ (referring to Figures 1 & 3). In other words,

$$v_i'(t) - v_i(t) = K(t) \sqrt{y_i^2 + z_i^2}, \quad i=1,2,\dots,16 \quad (B-1)$$

with $K(t)$ a function of t only. Equation (B-1) implies that

$$K(t) \sum_{i=1}^{16} \sqrt{y_i^2 + z_i^2} = \left(\sum_{i=1}^{16} v_i'(t) \right) - 16 v_i(t) \quad (B-2)$$

Equation (B-2) and (3-2) further imply that

$$K(t) = \frac{16 \bar{v}(t)}{\sum_{i=1}^{16} \sqrt{y_i^2 + z_i^2}} (1 - x_1(t)) \quad (B-3)$$

with
$$x_1(t) = \frac{v_1'(t)}{\bar{v}(t)} \quad (B-4)$$

that Equation (3-3) is the result of Equations (B-1) and (B-3) and the fact

$$\frac{16}{\sum_{i=1}^{16} \sqrt{y_i^2 + z_i^2}} = 0.416 \quad (B-5)$$

Finally, the values of $x_i(t)$ ($i=1, 2, \dots, 16$) as given by Equation (3-3) for $x_1(t) = 1.2, 1.6$ and 2.0 are shown in Figures 20, 21 and 22, respectively.

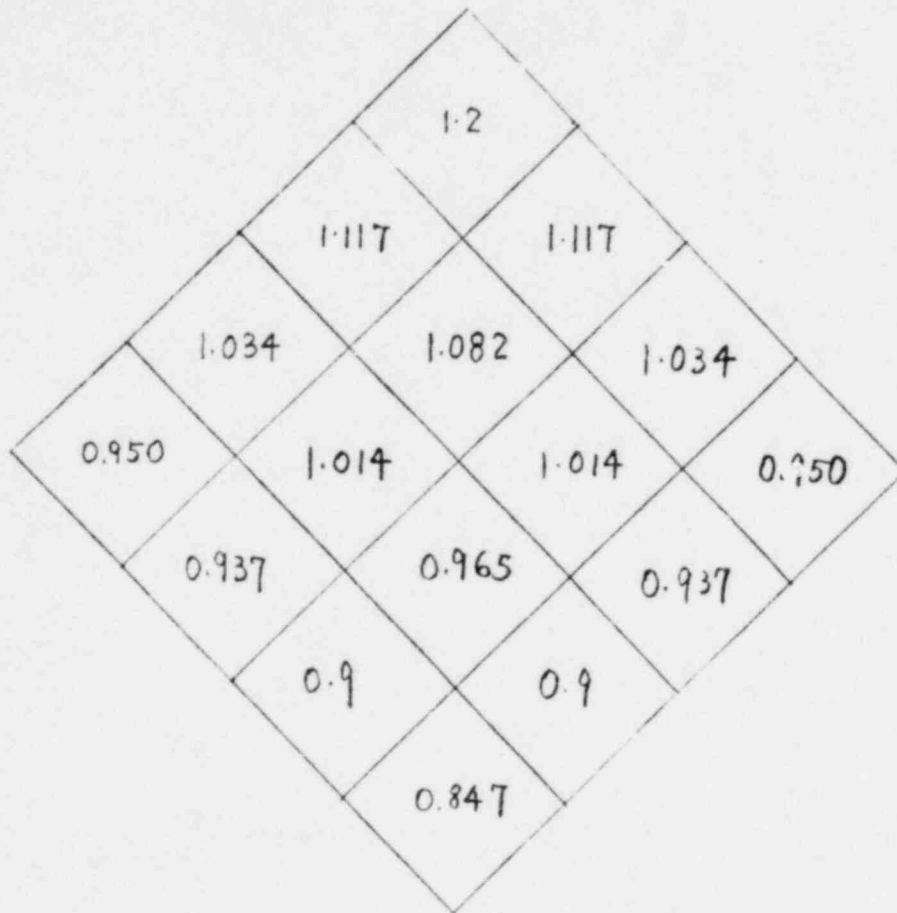


FIG. 20. VALUES OF $\chi_i(t)$ ($i=1, 2, \dots, 16$) if $\chi_1(t)=1.2$

998 039

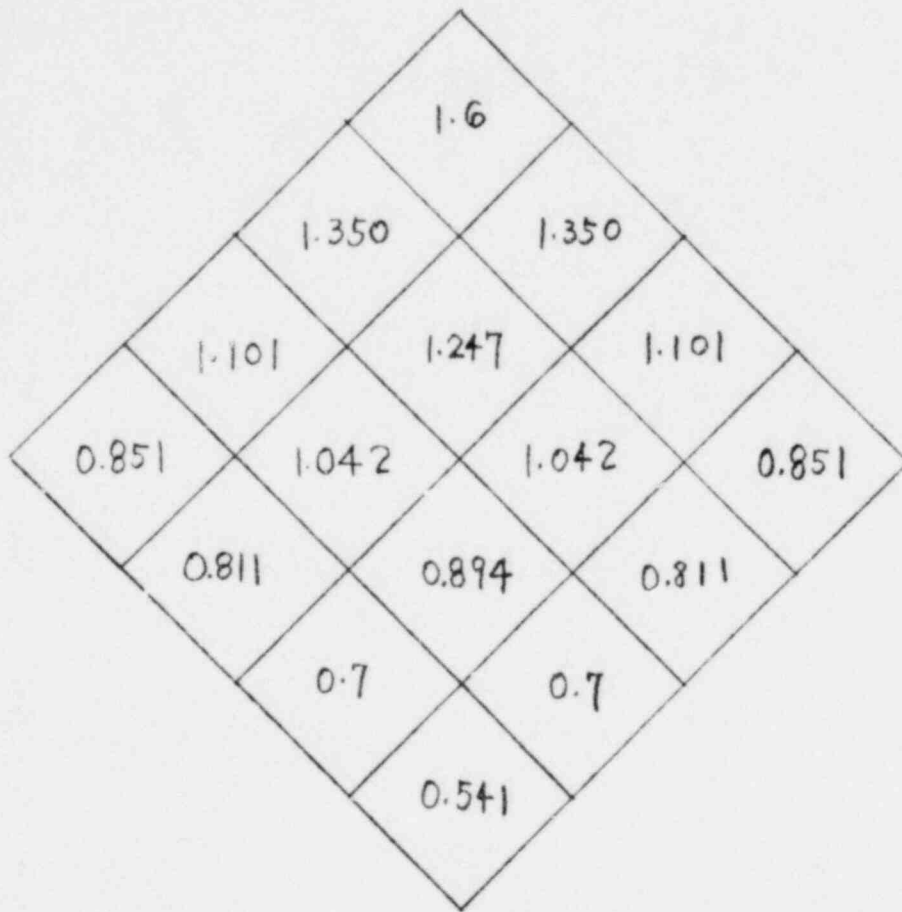


FIG. 21. VALUES OF $\chi_i(t)$ ($i=1, 2, \dots, 16$) if $\chi_1(t)=1.6$

998 040

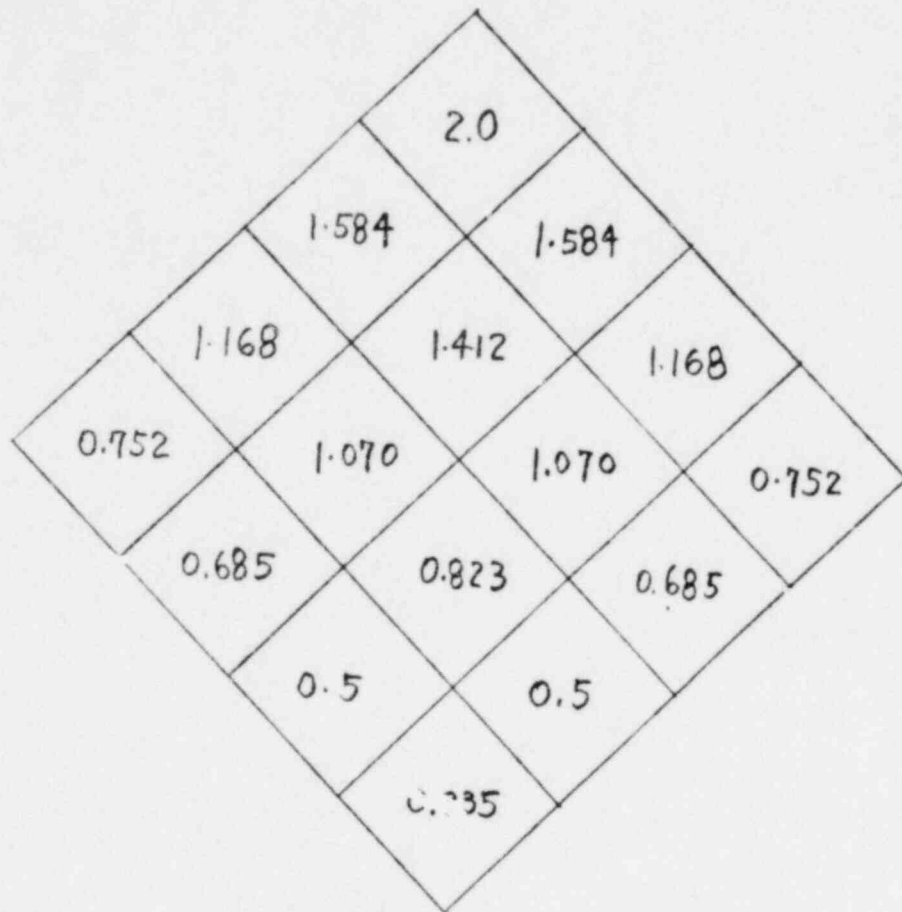


FIG. 22. VALUES OF $\chi_i(t)$ ($i = 1, 2, \dots, 16$) if $\chi_1(t) = 2.0$.

998 041

REFERENCES

1. S. C. CHANG, Potential Influence of Crossflow and Radiation Heat Transfer on LOFT LOCA Behavior, LTR 1111-53 (August, 1978).
2. M. M. Giles, MOXY/SCORE-version 4, Letter to T. R. Yackle, EG&G Interoffice Correspondence (August 22, 1977). This version is filed with INEL Configuration Control under the number H00147IB. The input deck for current MOXY/SCORE calculations is files with INEL Configuration Control under the number H00896IB.
3. R. L. Benedetti, L. V. Lords, and D. M. Kiser, SCORE-EVET: a Computer Code for the Multidimensional Transient Thermal-Hydraulic Analysis of Nuclear Fuel Rod Arrays, TREE-NUREG-1133 (February, 1978).
4. R. E. Collingham and J. Yates, Hydraulic Performance of LOFT Fuel Assemblies, XN-75-61 (June 30, 1976).

998 U42